UNIVERSITY OF MINNESOTA
ST. ANTHONY FALLS HYDRAULIC LABORATORY
LORENZ G. STRAUB, Director

Technical Paper No. 37-B

Longitudinal Motions and Stability of Two Hydrofoil Systems Free to Heave and Pitch in Regular Waves

by

J. M. WETZEL and W. H. C. MAXWELL

Prepared for
DAVID TAYLOR MODEL BASIN
Department of the Navy
Washington, D. C.
under
Bureau of Ships Fundamental Hydromechanics Research Program
SR-009-01-01
Office of Naval Research Contract Nonr 710(30)

December 1961
Minneapolis, Minnesota

ERRATA FOR TECHNICAL PAPER NO. 37-B

p. vii - line 25:

$J_1(\frac{kb}{2})$ - Bessel function of <u>first</u> kind of order one and argument (kb/2)

p. ix - line 2:

θ - Rotation of towing arm, also argument of E.

p. 3 - line 6: "usually" for "uaully"

p. 43 - Equation (A-6):

$$Z(A_2 + i\,B_2) + \Psi(C_2 + i\,D_2) = E_2 + i\,F_2$$

p. 44 - line 1:

$$B_1 = (\frac{Xv}{V}\cos\varsigma)\,\Sigma\,\beta'$$

line 7:

$$B_2 = (\frac{Xv}{V}\cos\varsigma)\,\Sigma\,(\beta'\delta x)$$

p. 45 - Equation (A-7):

$$\frac{|Z|}{a} = \frac{1}{a}\cdot\frac{\sqrt{A_6^2 + B_6^2}}{A_3^2 + B_3^2}$$

line 16:

$$\text{Also } \Psi = \frac{A_5 + i\,B_5}{A_3 + i\,B_3} = \frac{A_7 + i\,B_7}{A_3^2 + B_3^2}$$

p. 46 - Equation (A-12):

$$\ddot{\Psi} + A_9\dot{\Psi} + B_9\Psi + C_9\dot{Z} + D_9 Z = E_9 \sin \nu t + F_9 \cos \nu t$$

p. 47 - lines 7 through 14: the factors (1/m), (1/IV), and (1/I) multiply the quantity following Σ

line 21: $a_3 = A_8B_9 + B_8A_9 - D_8C_9 - D_9C_8$

p. 49 - Equations (A-16) and (A-17)

$$\ddot{z} = P_1\alpha_f + P_2\alpha_a + P_3\beta_f + P_4\alpha_f\beta_f$$

$$\ddot{\Psi} = Q_1\alpha_f + Q_2\alpha_a + Q_3\beta_f + Q_4\alpha_f\beta_f$$

ERRATA FOR TECHNICAL PAFER NO. 37-B
(continued)

p. 49 - Equation (A-19):

$$\text{where } R_3 = \mp \frac{\omega e^{-kd_a} \cos k\ell}{V} \quad \text{and} \quad R_4 = \pm \frac{\omega e^{-kd_a} \sin k\ell}{V}$$

p. 50 - line 11:

Insert P_3 before $\dfrac{[n_9 \beta_f]}{n_9}$

lines 11 through 14: for p_1, p_2, p_3, p_4 read P_1, P_2, P_3, and P_4.

lines 16 through 20:

$$[n_2 z]' = \int \left\{ \frac{n_2 P_1}{n_7} [n_7 \alpha_f] + \frac{n_2 P_2}{n_8} [n_8 \alpha_a] + \frac{n_2 P_3}{n_9} [n_9 \beta_f] + \frac{100\, n_2 P_4}{n_7 n_9} \cdot \frac{[n_7 \alpha_f][n_9 \beta_f]}{100} \right\} dr$$

$$= \int \left\{ p_{15} g_{15} [n_7 \alpha_f] + p_{16} g_{16} [n_8 \alpha_a] + p_{17} g_{17} [n_9 \beta_f] + p_{18} g_{18} \cdot \frac{[n_7 \alpha_f][n_9 \beta_f]}{100} \right\} dr$$

UNIVERSITY OF MINNESOTA
ST. ANTHONY FALLS HYDRAULIC LABORATORY
LORENZ G. STRAUB, Director

Technical Paper No. 37-B

Longitudinal Motions and Stability of Two Hydrofoil Systems Free to Heave and Pitch in Regular Waves

by

J. M. WETZEL and W. H. C. MAXWELL

Prepared for
DAVID TAYLOR MODEL BASIN
Department of the Navy
Washington, D. C.
under
Bureau of Ships Fundamental Hydromechanics Research Program
SR-009-01-01
Office of Naval Research Contract Nonr 710(30)

December 1961
Minneapolis, Minnesota

PREFACE

The studies described in this report are related to the analytical and experimental determination of the motions of hydrofoil craft in regular seas. These studies may be considered as an extension of earlier work done first at the David Taylor Model Basin and followed by work at the St. Anthony Falls Hydraulic laboratory. The previous work at this Laboratory was concerned with one particular hydrofoil configuration, a tandem V foil system. The current report describes tests with two other configurations, a V foil forward, flat foil aft system, and a system utilizing V foils fore and aft with a flat foil near the center of gravity.

The tests were carried out in the period August 1, 1960, to January 31, 1962, under the Bureau of Ships Fundamental Hydrodynamics Research Program, SR-009-01-01, administered by the David Taylor Model Basin; Office of Naval Research Contract Nonr 710(30).

The report was critically reviewed by C. E. Bowers. Experimental work was carried out mainly by John Almo, F. R. Schiebe, W. Parmenter, and F. Thomas. W. H. C. Maxwell was primarily responsible for the analog computer work. Preparation of the manuscript for publication was done by Marjorie Olson under the direction of Loyal Johnson.

A B S T R A C T

Experimental measurements were made of the motions of two hydrofoil configurations free to heave and pitch in regular waves. The two configurations consisted of 1) a dihedral (V) foil forward, flat foil aft, and 2) dihedral (V) foils both fore and aft, and a flat foil near the center of gravity. The motions were measured in both head and following seas for a variety of wave characteristics and two towing velocities. The experimental results were compared with quasi-steady linear and nonlinear theory, and also unsteady linear theory. In general, agreement with the quasi-steady linear theory was satisfactory, although some improvement in the correlation was obtained by considering the effects of unsteadiness. Nonlinearities had little effect on the amplitudes of the oscillatory motions. The major effect of the nonlinearities was to produce a steady downward component of heave. The measured component was in most cases greater than that derived from analog computer solutions of the nonlinear equations.

Experimental investigation of the inherent stability of both configurations in smooth water indicated that the damping was greater than predicted by the quasi-steady linear theory.

CONTENTS

LIST OF ILLUSTRATIONS

LIST OF SYMBOLS

A_o - First order approximation of wave orbital motion exponential decay factor, $\frac{1 - e^{-kd}}{kd}$ for V foils, $e^{-k\xi}$ for flat foils.

a - Wave amplitude.

B_o - $c_o \rho b V^2 \cot \mu$.

B' - $c' \rho b V^2 \cot \mu$.

b - Foil chord.

$C(\frac{\nu b}{2V})$ - Theodorsen function with argument $\nu b/2V$.

c - Wave celerity.

c_o - Lift coefficient for foil in smooth water.

c' - Lift curve slope.

D - Complex function that applies to forces due to unsteady foil motion.

d - Depth of submergence of V foil apex in smooth water.

E - Complex function that applies to forces due to unsteady orbital motion.

e - Distance from flat mid-foil to center of gravity of craft in VFV configuration.

F_o - $1/2\ \rho V^2 c c_o$.

F' - $1/2\ \rho V^2 c c'$.

g - Acceleration of gravity.

I - Moment of inertia of craft.

I_T - Moment of inertia of towing arm.

i - $\sqrt{-1}$.

$J_o(\frac{kb}{2})$ - Bessel function of first kind of order zero and argument $(kb/2)$.

$J_1(\frac{kb}{2})$ - Bessel function of second kind of order one and argument $(kb/2)$.

k - $2\pi/\lambda$.

L - Lift.

ℓ - Distance from forward or aft foil to center of gravity of craft (also see e).

ℓ_T - Length of towing arm from pivot point.

m - Mass of craft.

m_1 - Analog computer circuit scale factors.

r - Computer time, St.

S - Analog computer time scale factor.

s - Flat-foil span.

T - Torque on towing arm.

T_2 - Towing arm correction factor.

t - Real time.

V - Craft velocity.

VF - V foil forward, flat foil aft configuration.

VFV - Tandem V foil with flat mid-foil configuration.

W - Craft weight, mg.

X - Modulus of D.

x - Distance from foil to craft center of gravity, either e or ℓ depending on configuration.

Y - Modulus of E.

Z - Heave displacement.

$\dot{Z}$ - Real heave velocity dZ/dt.

$\dot{Z}'$ - Machine heave velocity dZ/dr.

Z_i - Initial heave (at t = 0).

Z_o - Steady component of heave.

α - Instantaneous angle of attack.

β - Instantaneous depth of submergence.

β_o - $B_o d$ for V foils, $F_o s$ for flat foils.

β' - $B'd$ for V foils, $F's$ for flat foils.

Δ - Factor equal to 1 for V foils, 0 for flat foils.

δ - Factor equal to +1 for forward foil, -1 for aft foil.

ζ - Argument of D.

θ - Rotation of towing arm, also argument of ψ.

λ - Wave length.

μ - Dihedral angle.

ν - Frequency of encounter, $k(V \pm c)$.

ξ - Submergence of flat foil in smooth water.

ρ - Fluid density.

σ - Root of characteristic equation.

ϕ - Phase angle, subscripts indicate heave or pitch.

ψ - Pitch.

ψ_o - Steady component of pitch (trim).

$\dot{\psi}$ - Real pitch velocity $d\psi/dt$.

ψ' - Machine pitch velocity $d\psi/dr$.

Ω - Routh's discriminant.

ω - Circular frequency, $2\pi/t$.

∇ - Determinant.

Subscripts f, a - Indicate forward or aft foil.

Subscript m - Indicates maximum amplitude or mid-foil.

Symbols not included in this list are defined in the text.

LONGITUDINAL MOTIONS AND STABILITY OF TWO HYDROFOIL SYSTEMS FREE TO HEAVE AND PITCH IN REGULAR WAVES

I. INTRODUCTION

The rather extensive work on hydrofoils in the past has been directed toward results which would enable a designer to determine the forces acting on the foils, within engineering accuracy, and eventually to predict the stability and motions of a given hydrofoil configuration in smooth and rough water. Using available information, equations of motion have been developed by several investigators [1, 2, 3]* for various types of motion in regular seas. It was of interest to subject these theories to experimental verification as a means of determining the validity of the simplifying assumptions. Previous to tests conducted at this Laboratory, apparently the only systematic tests have been reported by Leehey and Steele [4] for three configurations and one craft velocity. An extension of this work for one particular configuration used by Leehey and Steele to a higher towing velocity and wider range of wave conditions is reported in Ref. [5]. The present report describes tests with the other two additional hydrofoil configurations and provides a comparison with available linear and nonlinear theory.

The investigations were sponsored by the Bureau of Ships Fundamental Hydrodynamics Research Program, SR-009-01-01, administered by the David Taylor Model Basin, Office of Naval Research Contract Nonr 710(30).

II. THEORETICAL CONSIDERATIONS

Several investigators have developed theories predicting the longitudinal motions (heave and pitch) of a hydrofoil craft in regular seas. Weinblum [1] presented an approximate theory, employing linearization to simplify the solution. In comparing the experimental data with this theory, it was found [4] that the theory predicted motions considerably in excess of the measured motions. Ogilvie [2] modified the theory by considering the attenuation of wave orbital velocity with depth and obtained more realistic results. He considered both quasi-steady and unsteady flows in the solution of the linear and nonlinear equations of motion. The solution of the quasi-steady nonlinear

---

*Numbers in brackets refer to the List of References on p. 15.

coupled equations gave indication of a steady downward displacement of both heave and pitch, this displacement increasing with increasing wave amplitude and also for following seas.

As Ogilvie's theory was of most consequence for the purposes of this report, the assumptions made will be mentioned at this point to perhaps prepare the reader for the discussion of results to follow in a later section. A more complete description of the theory and the solutions of the equations of motion are presented in Appendix A. The theory was restricted to a craft free to heave and pitch, and rather extensive use was made of classical aerodynamic theory. In setting up the equations of motion, several assumptions were necessary in order to calculate the lift forces on each of the foils of the system. Some of these assumptions were later removed and their effects studied in considerable detail. The basic simplifying assumptions were as follows:

(1) The lift is proportional to the product of the instantaneous angle of attack and the instantaneous horizontal projection of the submerged foil area.

(2) The wave length is much greater than the foil chord.

(3) The slope of the lift curve is constant.

(4) The downwash and waves generated by the forward foil may be neglected.

(5) The horizontal component of the wave particle motion is small compared to the craft speed.

(6) The distance from the center of gravity of the craft to the foil is much greater than the foil chord.

(7) The lift on a flat foil is independent of submergence.

A brief discussion of several of these assumptions may be in order at this time. The first assumes a quasi-steady computation of the lift. This restriction is later modified to take into consideration unsteadiness effects due to changing of the angle of attack and nonuniformity of the velocity over the chord. The instantaneous horizontal projection of the foil area is important only in the case of the dihedral surface-piercing foil systems (also referred to as V foils), as the area of a flat foil is independent of the

changes in submergence created by the wave system and the resulting craft motions. The unsteadiness associated with the changing area of the dihedral foil was not taken into consideration due to the complexity of the flow in the region of the surface and the lack of any similar effect in classical aerodynamic theory.

The lift curve slope is uaually constant for a given aspect ratio and profile over a relatively wide range of attack angles. However, in the case of a dihedral, surface-piercing foil moving through waves, the aspect ratio is a function of the instantaneous submergence. The lift curve slope will therefore change correspondingly. To avoid the difficulty associated with this effect, the lift curve slope corresponding to the submergence of the foil in a level flying position was used in the calculations. A slight change in lift curve slope was also noted for low velocities, although at the higher speeds a constant value was approached and little error would perhaps be introduced by neglecting this effect.

The effect of downwash and waves generated from the forward foil has been partially taken into consideration through the methods used in the experimental phase of the program. The foils of the craft were adjusted so that the craft would fly in a level position for a given submergence of the foils. This required a different angle of attack for the forward and aft foils. The effect of the waves on the downwash has not been considered at this point.

Referring to the definition sketch for an arbitrary foil system shown in Fig. 1, the equations of motion are written in the following form:

$$m\ddot{Z} = \Sigma L - W \tag{1}$$

$$I\ddot{\psi} = \Sigma L \delta x \tag{2}$$

where m = mass of craft,

Z = heave, positive upward,

ΣL = sum of lifts of all foils,

W = weight of craft,

I = moment of inertia of craft,

ψ = pitch, positive bow-up,

x = distance from center of gravity to center of pressure of each foil, and

δ = +1 for foil forward of craft center of gravity; -1 for foil aft of craft center of gravity.

It should be noticed that the drag of the foils has been neglected in the second equation. As the drag force tends to create an additional moment about the center of gravity, it is partially taken into consideration by adjusting the craft to fly at an equilibrium position (zero trim) in smooth water.

The lift forces will depend on the angle of attack, and in the case of the dihedral foils, on the depth of submergence. Therefore, it is obvious [Appendix A, Eqs. (A-16) through (A-20)] that the lift will be dependent on both pitch and heave, as well as heave and pitch velocities. Thus, the equations of motion are coupled through these terms, the degree of coupling in part being determined by the type of hydrofoil configuration or the combination of hydrofoils used for a particular system. As an example, if a symmetrical system is considered, i.e., one with two identical foils, Eq. (2) will be a differential equation containing the pitch ψ and its derivatives only. Pitch will be coupled into the heave equation, however. An examination of the detailed equations presented in the Appendix will more completely reveal the strength of the coupling for various systems.

Some experimental work has also been reported on the forces on dihedral foils in regular waves [6]. These tests were conducted using foils restrained in both heave and pitch. It was found that for the larger wave amplitudes, a considerable amount of second harmonic distortion was present in the oscillatory lift force. This component was in most cases considerably larger than that predicted by nonlinear theory [2]. Associated with the distortion was a slight change in the average lift as compared to the lift on the foil passing through smooth water. Experiments with the two identical dihedral foils in tandem have shown that the performance ratio of the aft foil may be increased over the value for the foil alone for a certain separation of foils. The foil separation for maximum performance depends on the velocity of the craft, increasing for increasing speed. This effect is currently being investigated for flat foils in tandem under another contract. The performance ratio of the aft foil in a tandem configuration moving through a regular wave train is also under study.

III. EXPERIMENTAL APPARATUS AND PROCEDURE

A. Test Facility

The tests were conducted in the multi-purpose channel which is 9 ft wide, 6 ft deep, and 220 ft long. The water depth was maintained at 4.5 ft. This facility is equipped with a self-propelled towing carriage and a wave generator. The towing carriage is capable of attaining accurately controlled speeds in either direction up to a maximum of 25 fps. Speeds of 5 and 10 fps were used for the tests described in this report. The wave generator is capable of producing waves of various lengths and amplitudes, up to a maximum of about 18 ft long and 2 ft high. Waves down to about 2.0 ft in length can be generated satisfactorily. Below this value, the waves become unstable with increasing distance from the generator, thereby reducing the length of the test run. For this reason wave lengths shorter than 2.0 ft were not used in the tests. A permeable beach absorber was located at the opposite end of the channel to minimize wave reflections. A more complete description of the facility is presented in Ref. [7].

B. Hydrofoil Craft

The hydrofoil craft was obtained on loan from the sponsor and was basically the same as previously used in the experiments by Leehey and Steele. Modifications were made to the pitch and heave indicating systems of the original craft. With these changes, it was possible to measure heave and pitch independently of each other by use of linear differential transformers. Structural bracing was also added to the craft and the towing arm resulting in slight changes in moment of inertia and mass. A sketch of the original and revised systems is shown in Fig. 2. The movable weights were used to balance the craft about the axles and also to adjust the moment of inertia of the craft to predetermined values. The centers of gravity of the towing arm and craft were located at their pivot points. The same basic framework of the towing arm and craft, with the exception of the foil configurations, was used in the previous tests described in Ref. [5].

Two basic hydrofoil configurations were investigated:

(1) "V" foil forward, flat foil aft; and

(2) "V" foils forward and aft, flat foil near center of gravity.

TABLE I

SUMMARY OF CRAFT CHARACTERISTICS

Symbol	Characteristics at Equilibrium Flight Condition	Configuration			
		VF-5	VF-10	VFV-5	VFV-10
m	mass, slugs	0.1205	0.1205	0.151	0.151
I	moment of inertia, slugs ft^2	0.176	0.176	0.208	0.208
$\ell_f = \ell_a$	c.g. to fwd. or aft foil, ft	1.5	1.5	1.5	1.5
e	c.g. to mid-foil, ft	-	-	0.27	0.27
c	flat foil chord, ft	0.167	0.167	0.167	0.167
b	V foil chord, ft	0.167	0.167	0.167	0.167
s	flat foil span, ft	1.04	1.04	1.04	1.04
c_{o_f}	lift coeff. fwd. foil	0.458	0.175	0.65	0.38
c_{o_a}	lift coeff. aft foil	0.461	0.115	0.26	0.17
c_{o_m}	lift coeff. mid-foil	-	-	0.20	0.10
c'_f	lift slope fwd. foil	4.20	3.58	3.58	3.58
c'_a	lift slope aft foil	4.90	4.90	3.58	3.58
c'_m	lift slope mid-foil	-	-	4.73	4.73
μ_f	dihedral fwd. foil, degrees	45	45	45	45
μ_a	dihedral aft foil, degrees	0	0	45	45
μ_m	dihedral mid-foil, degrees	-	-	0	0
d_f	submergence fwd. foil, ft	0.523	0.342	0.342	0.342
d_a	submergence aft foil, ft	0.544	0.385	0.342	0.342
ξ	submergence mid-foil, ft	-	-	0.385	0.385

In all cases, the foils were of 2-in. chord, and machined from aluminum to a Wright 1903 section. The V foils had a 45-degree dihedral angle. The flat foil was supported by two streamlined struts located at the ends of the foil.

The weights and moments of inertia of the craft were adjusted to be generally the same as for the original craft as used by Leehey and Steele. The moment of inertia was measured by the method described by Reiss [8].

A summary of the craft characteristics is presented in Table I for both configurations. As each configuration was utilized for two velocities

both in head and following seas, a systematic notation has been adopted that will be followed throughout the report. A combination of letters and numbers designate the foil arrangement, direction of travel with respect to waves, and towing velocity. For example, VF-H-5 refers to the V foil forward, flat foil aft arrangement moving in head seas with a towing velocity of 5 fps. The combination VFV-F-10 refers to the V foils forward and aft, flat mid-foil configuration moving in following seas with a towing velocity of 10 fps.

C. Test Procedure

The wave profile was measured from the moving carriage with a sonic surface wave transducer as developed at this Laboratory [9]. The sonic transducer greatly reduced difficulties in wave profile measurement previously created by dust on the water surface or by towing a probe through the water. The sonic head was mounted directly opposite the center of gravity of the craft to reduce the effort in determining the phase relationship between the waves and craft motions. The measurements of carriage speed, heave, pitch, and wave profile were recorded with a 4-channel Sanborn recorder. The wave length was calculated from the known period of the generator paddle.

Force measurements were made in smooth water at 5 and 10 fps to establish the lift curve slopes and steady-state lift coefficients required in the theoretical analysis.

The craft was adjusted to fly at a predetermined equilibrium position that corresponded to a given submergence of the foils. The desired attitude was that of zero trim, or with the longitudinal axis of the craft parallel to the water surface. It was found that to attain this attitude the angles of attack on the forward and aft foils were generally different, thus partially accounting for the downwash effects and the bow-down pitching moment created from the drag forces not considered in the theory. Waves were generated with lengths from 2 to 12 ft and amplitudes from 0.0125 to 0.1875 ft. It was not possible to generate the shorter waves at the larger amplitudes as the waves would become unstable at a relatively short distance from the wave generator. The wave length in following seas was limited by the wave length at which the craft would crash.

In general, the craft was supported at its equilibrium position, and released into the waves after a constant towing velocity was attained.

In some cases, the craft was permitted to reach its equilibrium position in a section of essentially smooth water before meeting the oncoming waves. A similar procedure was also used in following seas. In the latter instance, the wave generator was stopped, and after a suitable period of time the craft took off in the smooth water and overtook the waves. To prevent damage of the craft by crashing in following seas, stops were provided as close as possible to the water surface. Under normal conditions these stops did not interfere with craft motions.

D. Data Reduction

The following data were recorded: a) wave profile at the center of gravity of the craft, b) heave, c) pitch, and d) carriage velocity. The latter was useful in determining the actual length of the test run.

The raw data have been reduced in terms of the following dimensionless parameters:

$$\frac{Z_m}{a} = \text{heave amplification factor}$$

$$\frac{\psi_m \ell}{a} = \text{pitch amplification factor}$$

$$\frac{Z_o}{a} = \text{nondimensional steady heave}$$

$$\frac{\psi_o \ell}{a} = \text{nondimensional steady pitch}$$

where Z_m = maximum heave amplitude,

Z_o = steady heave displacement measured from the smooth water flight position,

ψ_m = maximum pitch amplitude,

ψ_o = steady pitch (trim) measured from smooth water flight trim,

ℓ = distance of forward or aft foils from center of gravity of craft, and

a = wave amplitude.

Phase relationships between the motions and the wave were also determined. The heave phase lead ϕ_Z is defined as the number of degrees of

wave cycle that the maximum upward heave of the craft leads the wave crest at the center of gravity of the craft. The pitch phase lead $\phi_{\downarrow}$ is the number of degrees of wave cycle that the maximum bow-up pitch leads the crest of the wave at the center of gravity of the craft.

A typical test record is shown in Fig. 3. The magnitude of the steady pitch appears to exceed that of the steady heave, although this is due to the different calibration of the heave and pitch channels. The steady heave actually is much greater than the steady pitch.

Some difficulties were experienced in measuring the steady components of heave and pitch to the same degree of accuracy obtained in the measurement of the oscillatory responses. A variation was found to exist in the equilibrium flight position of the craft in smooth water. As it was necessary to determine the magnitude of the steady displacement from the mean flight position, considerable scatter was introduced in the data. Whenever possible, the craft was permitted to attain an equilibrium position in smooth water before coming into contact with the regular wave train, and this equilibrium position was then used in determining the steady values. Steady components of pitch were in most cases very small, and the error inherent in the measuring system itself as well as the difficulties previously mentioned may result in the values being of little import. Thus, these measurements should be interpreted with this in mind.

IV. DISCUSSION OF RESULTS

A. Transient Responses

The longitudinal stability of both craft configurations has been determined from the linearized equations of motion (see Appendix A). The roots of the characteristic equations were found to be negative or complex with negative real parts indicating that all configurations were inherently stable longitudinally. The purely real roots were, in all cases, of large magnitude, indicating that the responses associated with them were very rapidly damped. The large negative real roots were therefore neglected in comparison with the complex roots, which resulted in oscillatory responses.

Practically, it was difficult to obtain heave responses for zero initial pitch displacement, or pitch responses for zero initial heave displacement. Consequently, the transients were obtained for both an initial heave and an initial pitch displacement, thus introducing coupling.

The theoretical responses were computed using the measured initial heave and initial pitch (Z_i and ψ_i), taking account of the sign convention defined in Section II. This, in some cases (e.g. the pitch responses for VF-5 and VF-10), caused the initial value to be exceeded at a later time, as a consequence of the coupling effect.

From a comparison of the measured and theoretical responses (Figs. 4 and 5) it is seen that the theory is conservative. Note that the scale of the nondimensional pitch response for the VF-10 configuration differs from that of the other configurations. The motions were damped more rapidly than the theory predicted, although in some instances the measured amplitudes exceeded the theoretical amplitudes (e.g. pitch response for VF-10). This indicated that there may be stronger coupling between the heave and pitch responses than was predicted by theory.

In the case of the VFV configuration the measured damping so exceeded the theoretical damping that an oscillatory response was not obtained.

The results are in general agreement with the findings of Leehey and Steele, namely that the theory underestimates the damping obtained in practice.

B. Oscillatory Motions

Data taken for a range of wave lengths and amplitudes were obtained for the VF and VFV configurations in head and following seas. These data were compared with the quasi-steady linear, quasi-steady nonlinear, and unsteady linear solutions discussed in detail in Appendix A. The results are shown in Figs. 6 through 17. For any particular wave length, tests were conducted for a series of amplitudes and the magnitudes of both the pitch and heave amplification factors in general appeared to increase with decreasing wave amplitude. This effect was masked to some extent by experimental scatter, particularly where the magnitudes of the parameters were small.

In the initial work all three theoretical solutions were obtained. It is evident, however, from Figs. 6 through 9 that the three solutions are in fairly close agreement. In general, the unsteady linear solution appears to agree best with the measured values, the quasi-steady linear solution being the least satisfactory. The latter solution was, therefore, not retained for the remaining work. In the case of the VFV configuration in head and following seas, the quasi-steady nonlinear computation was not obtained because

of insufficient time and funds. Only the unsteady linear calculation was completed.

For the VF configuration in following seas (Figs. 8 and 12) the agreement between theory and experiment at the higher wave lengths was not of the same order as for head seas, particularly for the heave amplification factor. Two effects may have contributed to this lack of agreement.

First, the variation of lift with submergence on a flat foil has been neglected in the theoretical analyses. This effect would probably increase in importance with wave length, particularly because of the larger magnitudes of the amplification factors at the longer wave lengths utilized. The effect of decreasing lift on the flat foil as the free surface is approached would be to reduce the heave response of the craft. This was borne out by the experimental results which fall well below the theoretical curves.

Secondly, for the VF-F-5 experiments considerable distortion of the pitch response occurred, due to the appearance of higher harmonics. This influenced the heave response to some extent due to the coupling effect, although the appearance of higher harmonics was not very marked in the heave response. A harmonic analysis of the pitch response was undertaken. The pitch amplification factor was then expressed in terms of the fundamental. For any particular wave length the relative influence of the higher harmonics showed scatter with amplitude. Except for the 3.5-ft wave length, for which the influence of the second harmonic increased with amplitude, there was no consistent relation between the higher harmonics and the amplitude. The results of the harmonic analysis are tabulated in Appendix C.

The analog solution for the VF-F-5 case was not very satisfactory at the longer wave lengths. It was necessary to slow the computer down considerably in order to satisfy the requirement that all machine variables remain under 100 volts. Combined with the low frequency of encounter occurring at longer wave lengths in following seas this led to a very slow rate of integration and introduced the probability of increased error in the solution.

In all tests the maximum wave length was limited to prevent crashing of the craft, which was particularly liable to occur in following seas for wave lengths greater than 4 ft at a velocity of 5 fps, or greater than 8 ft at a velocity of 10 fps. Crashing would occur at lower wave lengths for large wave amplitudes. Several reasons are suggested to account for this tendency to crash in following seas:

(1) The large amplitude of the transient response can cause swamping of the craft.

(2) The steady downward heave displacement increases with wave length in following seas.

(3) The orbital motion of the water particles introduces a tendency for the craft to nose into a wave crest in following seas [6].

In some experimental runs the craft was apparently swamped during the time the transient was acting but eventually recovered and flew in a displaced position when the transient had damped.

For the VFV configuration the heave and pitch amplification factors were similar in magnitude and form to those obtained for the VF configurations. The phase leads, however, showed no such similarity. The heave response for the VFV-F-5 tests showed much better correlation with theory than its VF counterpart.

It is noteworthy that maxima, minima, cusps, and discontinuities in the curves for the VF configuration (Figs. 6 through 13) were scattered throughout a range in wave length of 2.5 ft to 5 ft. In the VFV configuration (Figs. 14 through 17) the cusps, maxima, and discontinuities generally occur at a wave length of 3 ft, at which the wave length equals the foil spacing. One would expect that the pitch amplification would be a minimum at the 3-ft wave length and this was indeed the case. This was also found to be true for the case in which two identical V foils were tested in tandem [5].

C. Steady Components of Heave and Pitch (Trim)

The nonlinear solutions obtained on the analog computer for the VF configuration indicated that the oscillation of the heave and pitch would occur about a position displaced downward from the mean flight level in smooth water.

The experimental displacement proved difficult to measure and there was also a fair amount of scatter in the analog computer results. The difficulty derives from the small magnitude of the steady displacement. In general the steady heave displacement could be obtained with more accuracy than that of the pitch, primarily because of its greater magnitude. Consequently, only the steady heave displacements are presented in Fig. 18. The theoretical

curves shown have been smoothed in from the analog computer values. The relation between theory and experiment shows qualitative agreement and similar behavior was indicated for both velocities tested, the form differing for head and following seas.

No theoretical curves were available for the VFV configuration. The experimental results have, however, been presented in Fig. 19. Note that in Figs. 18 and 19 the downward steady heave was defined as positive.

Prior to the addition of bracing to the craft structure some difficulty was encountered in the measurement of the oscillatory heave response of the VF-H-10 configuration due to a "porpoising" motion of the craft. This took the form of an oscillatory heave response which was often of greater amplitude than the fundamental heave response and of longer period (3 to 7 sec). This behavior was negligible in the VF-H-5, VF-F-5, and VF-F-10 tests but was very marked in the smooth water runs at 10 fps, in which case it was clearly coupled to the pitch response.

The phenomenon also occurred to a much lesser extent in the VFV-H-5 tests and had even slighter influence in the VFV-F-5 tests, after the addition of bracing to the craft framework. At 10 fps the influence was even smaller in head seas and nonexistent in following seas. The behavior of the VFV configuration was, in this regard, similar to that of the tandem V foil configuration [5]. The VF configuration shows a marked difference in behavior in that the tendency to "porpoise" increased with velocity.

V. CONCLUSIONS

The following conclusions can be made, based on the experimental results described in this report:

(1) The experimental response to an initial disturbance is more heavily damped than indicated by theory.

(2) Coupling between heave and pitch responses may be stronger than indicated by theory.

(3) The St. Anthony Falls Hydraulic Laboratory data in general verify the quasi-steady theory developed by Ogilvie.

(4) The results are modified slightly by the consideration of unsteadiness effects. The improvement in correlation with

experimental values may not be sufficient to merit the additional computation involved in the unsteady theory.

(5) The steady nonlinear theory differs significantly from the quasi-steady linear and unsteady linear theories in that it predicts steady components of heave and pitch. These are obtained experimentally, although good correlation with the theory is not obtained, one of the reasons being the difficulty of measuring the experimental values to a sufficient degree of accuracy. Considerable experimental scatter results from the variation of the craft mean flight position, combined with the small magnitudes of the steady heave and pitch displacements. The nonlinear theory does not significantly improve the prediction of heave and pitch responses and their corresponding phase relations, when compared with the linear theories.

(6) Both configurations have a tendency to crash in following seas for the physical conditions used in these tests. This tendency is reduced with increasing craft velocity or frequency of encounter.

(7) It is felt that the theoretical correlation for the VF configuration could be improved by considering the effect of submergence on the lift of the flat foil. This effect is of less significance for the VFV configuration. In general, it is more apparent at longer wave lengths.

LIST OF REFERENCES

[1] Weinblum, G. P. Approximate Theory of Heaving and Pitching of Hydrofoils in Regular Shallow Waves. David Taylor Model Basin Report C-479. October 1954.

[2] Ogilvie, T. Francis The Theoretical Prediction of the Longitudinal Motions of Hydrofoil Craft. David Taylor Model Basin Report 1138. November 1958.

[3] Kaplan, Paul Longitudinal Stability and Motions of a Tandem Hydrofoil System in a Regular Seaway. Stevens Institute of Technology, Davidson Laboratory Report No. 517. December 1959.

[4] Leehey, Patrick and Steele, J. M. Jr. Experimental and Theoretical Studies of Hydrofoil Configurations in Regular Waves. David Taylor Model Basin Report 1140. October 1957.

[5] Wetzel, J. M. Experimental and Analytical Studies of the Longitudinal Motions of a Tandem Dihedral Hydrofoil Craft in Regular Waves. University of Minnesota, St. Anthony Falls Hydraulic Laboratory Technical Paper No. 30-B. April 1960.

[6] Wetzel, J. M. and Schiebe, F. R. Lift and Drag of Surface-Piercing Dihedral Hydrofoils in Regular Waves. University of Minnesota, St. Anthony Falls Hydraulic Laboratory Project Report No. 64. September 1960. (Not available for distribution)

[7] Straub, Lorenz G. and Bowers, C. E. The St. Anthony Falls Multi-Purpose Test Channel. University of Minnesota, St. Anthony Falls Hydraulic Laboratory Technical Paper No. 17-B. July 1956.

[8] Reiss, Howard R. A Procedure to Impart Specified Dynamical Properties to Ship Models. David Taylor Model Basin Report 986. March 1956.

[9] Killen, John M. The Sonic Surface-Wave Transducer. University of Minnesota, St. Anthony Falls Hydraulic Laboratory Technical Paper No. 23-B. July 1959.

[10] Fung, Y. C. An Introduction to the Theory of Aeroelasticity. John Wiley and Sons, Inc. 1955.

F I G U R E S

(1 through 19)

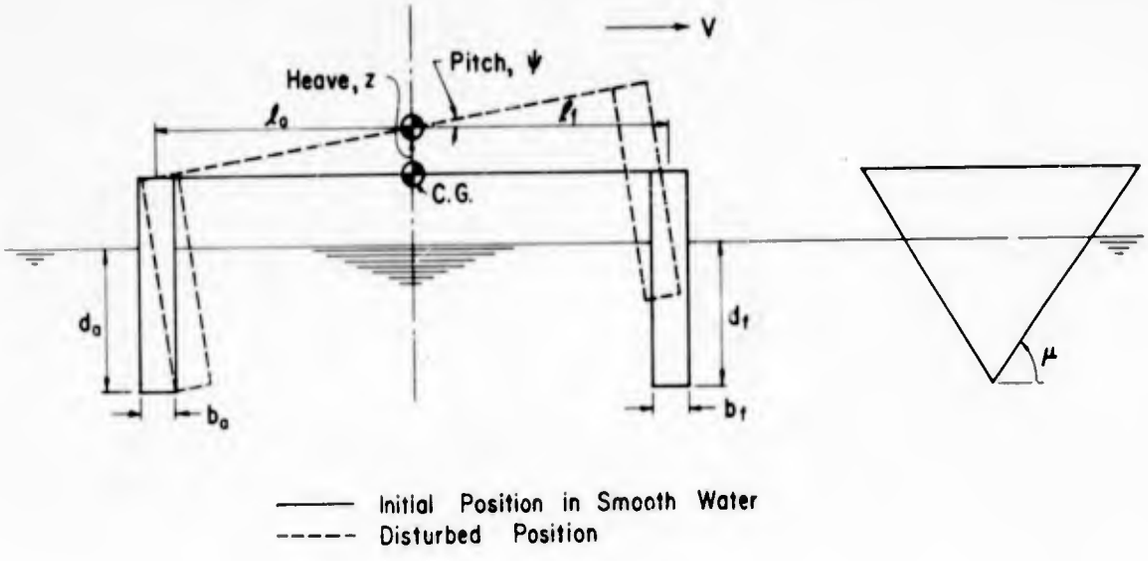

Fig. 1 - Defjnition Sketch of Craft Geometry

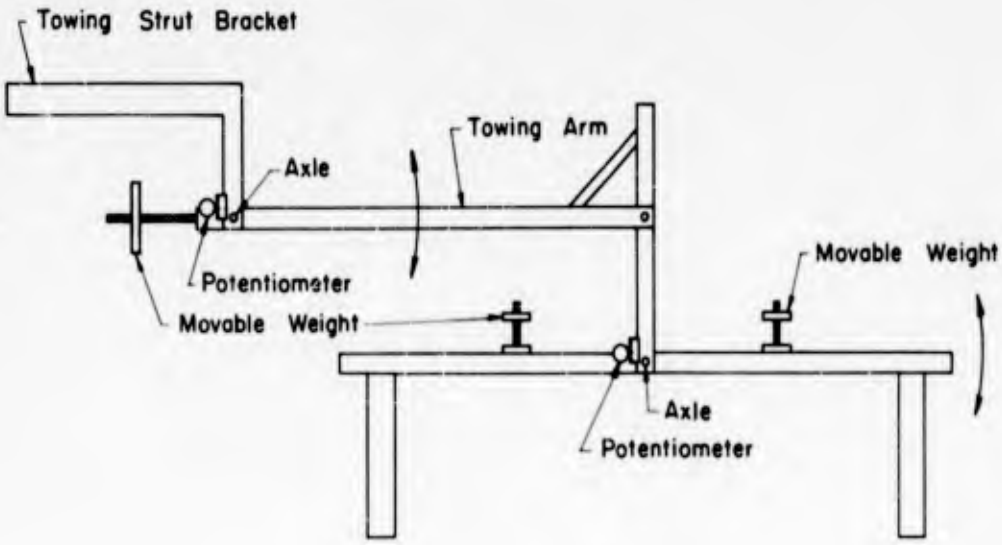

(a) Original (DTMB)

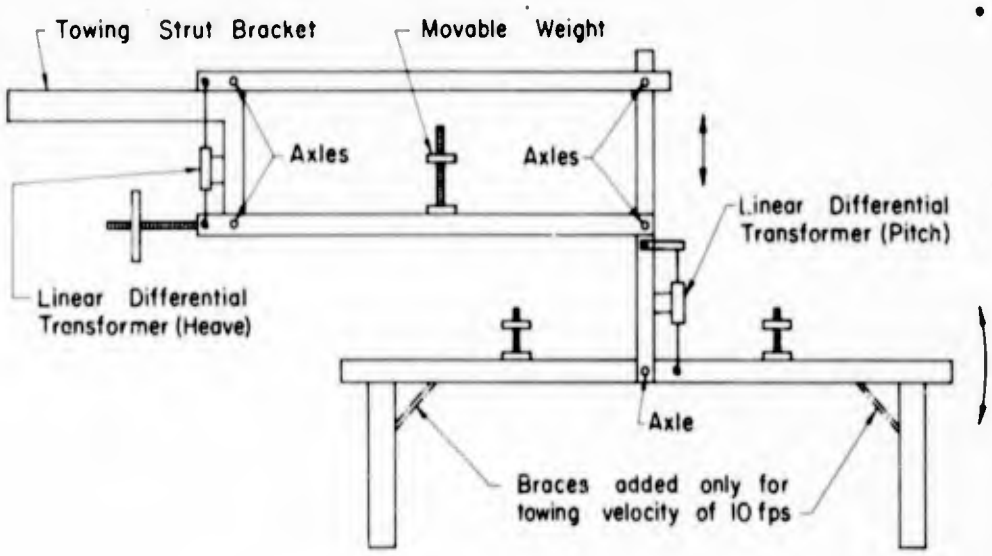

(b) Modified (SAFHL)

Fig. 2 - Instrumentation of Hydrofoil Craft

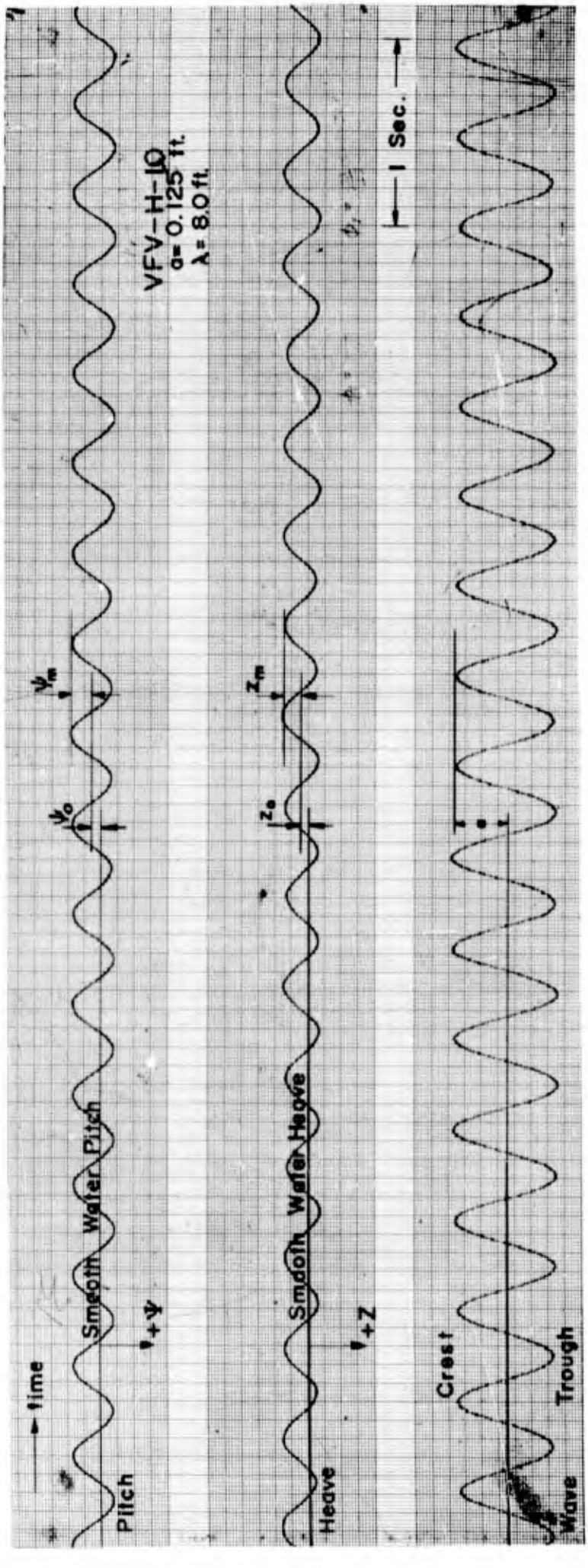

Fig. 3 - Typical Test Record

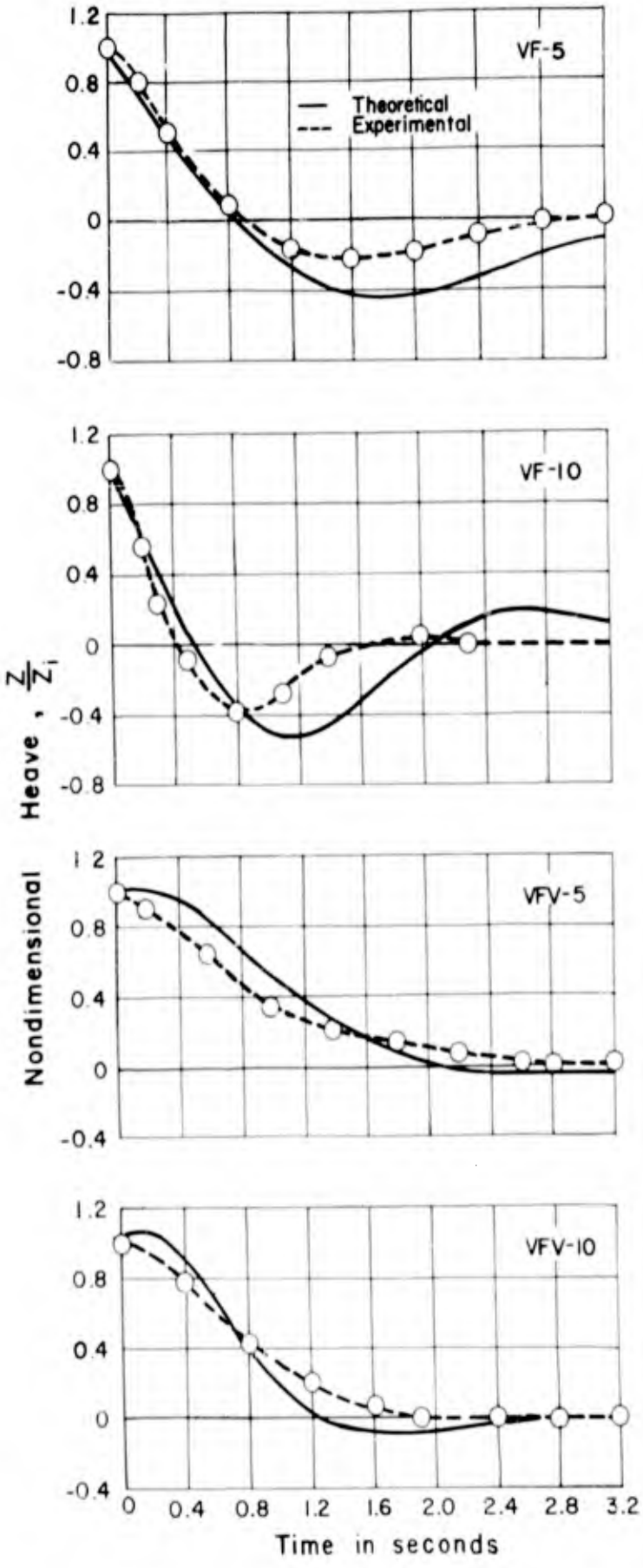

Fig. 4 – Transient Heave Response to Initial Displacement

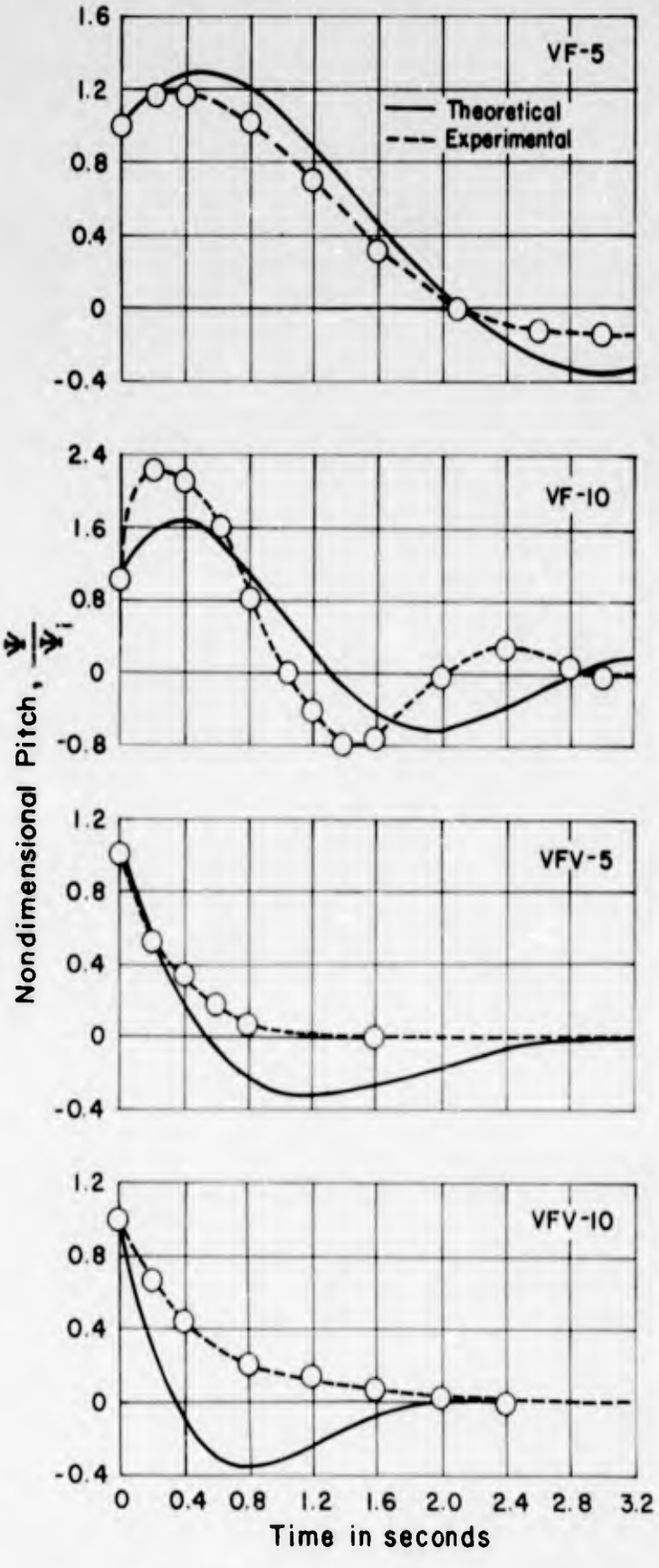

Fig. 5 - Transient Pitch Response to Initial Displacement

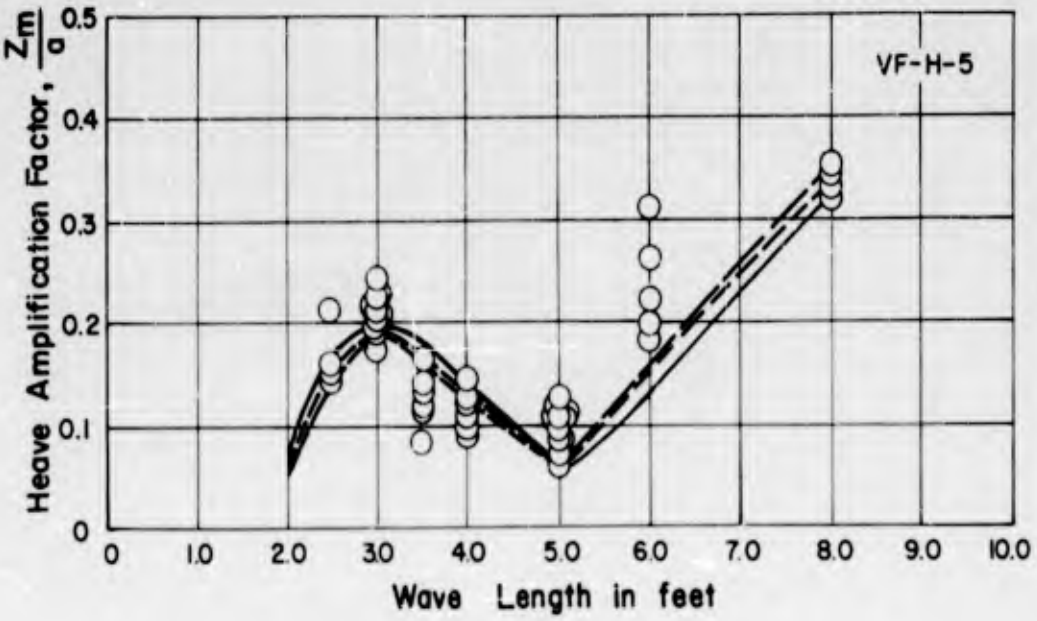

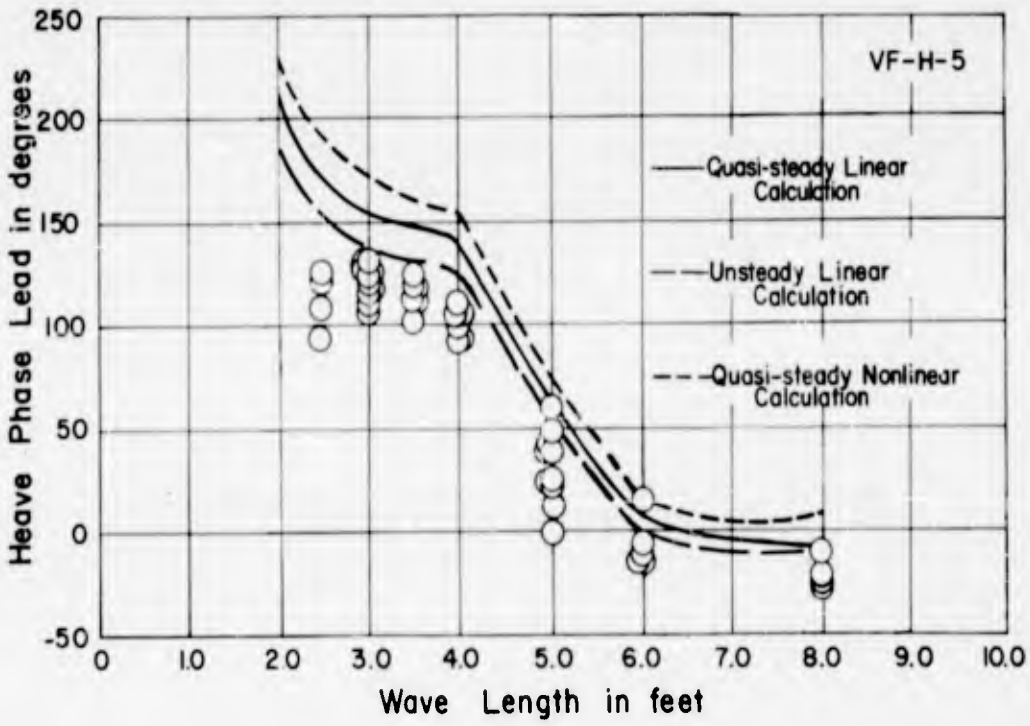

Fig. 6 - VF-H-5 Heave Response

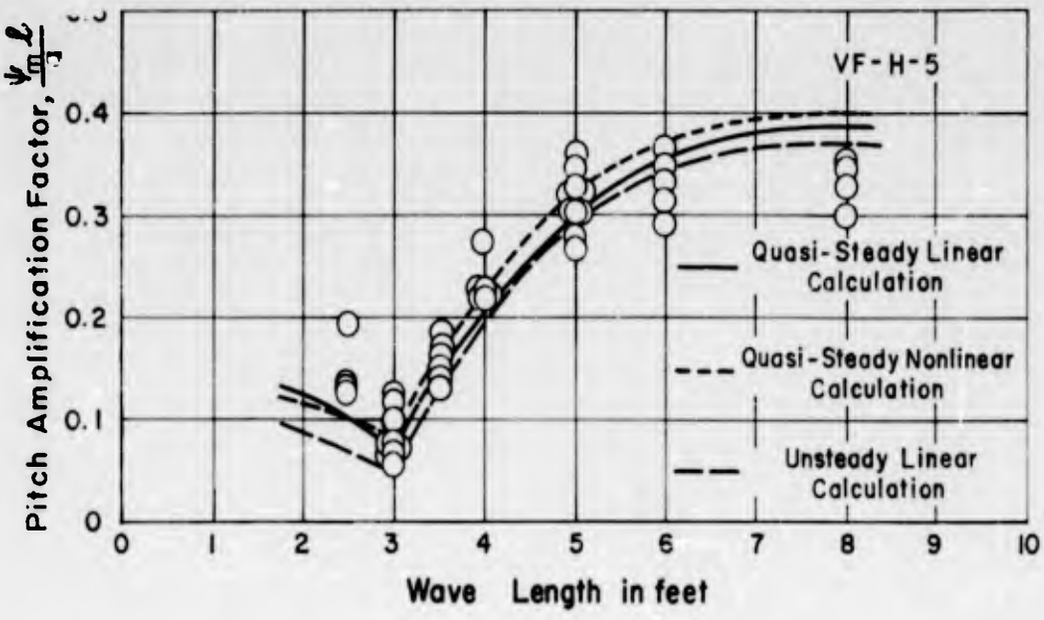

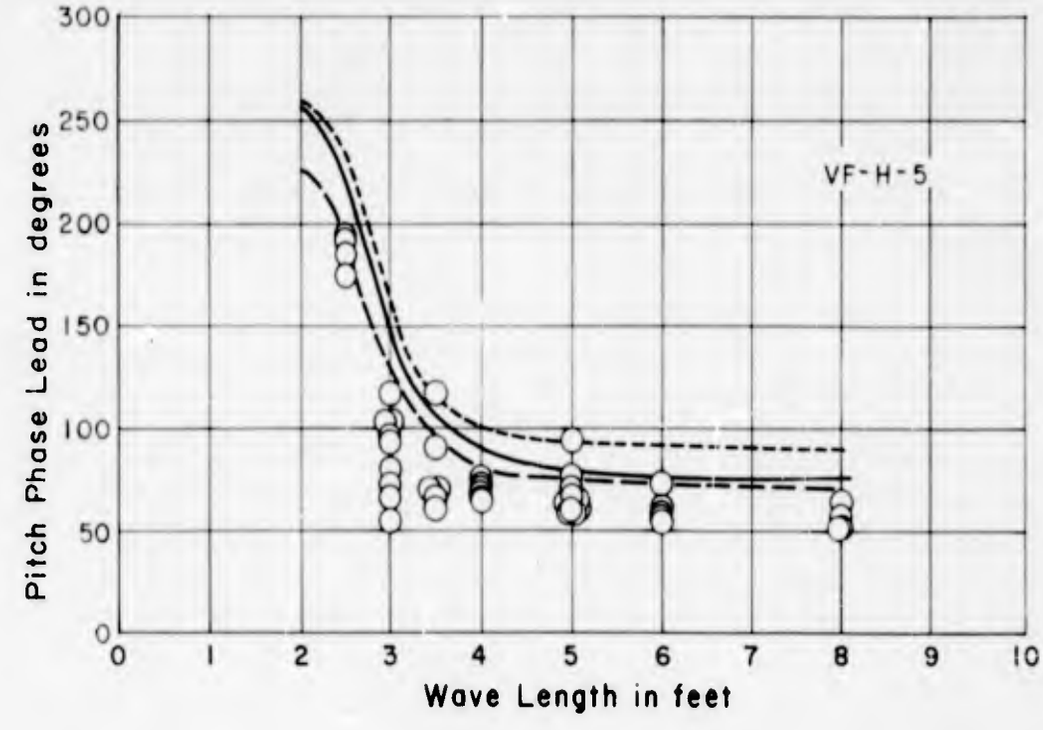

Fig. 7 - VF-H-5 Pitch Response

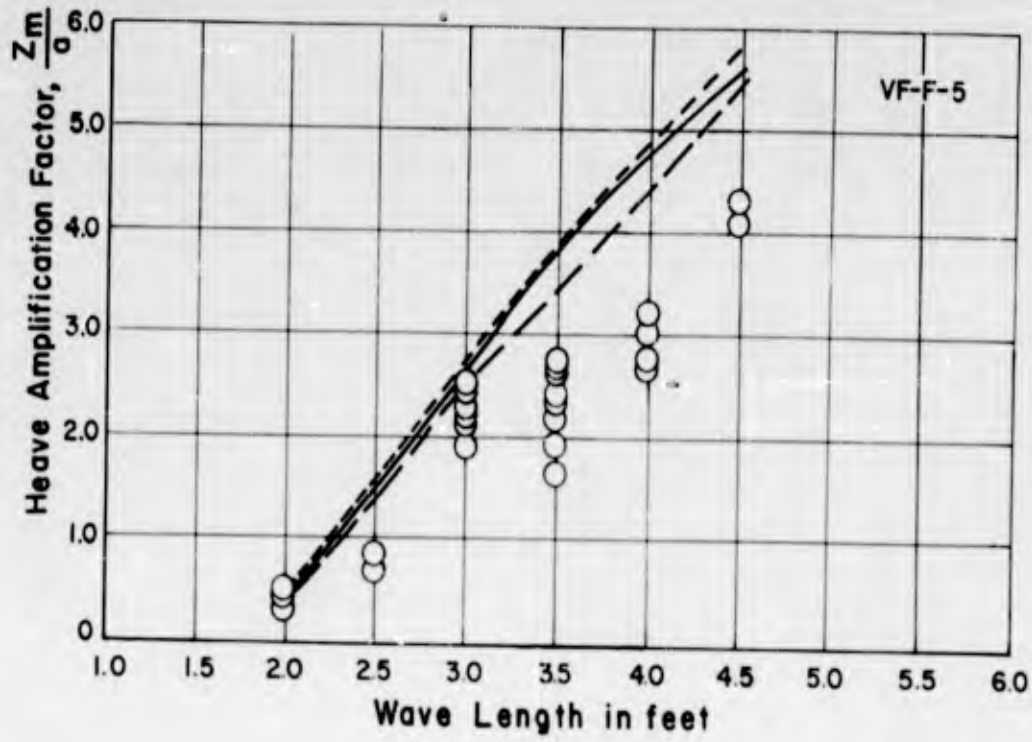

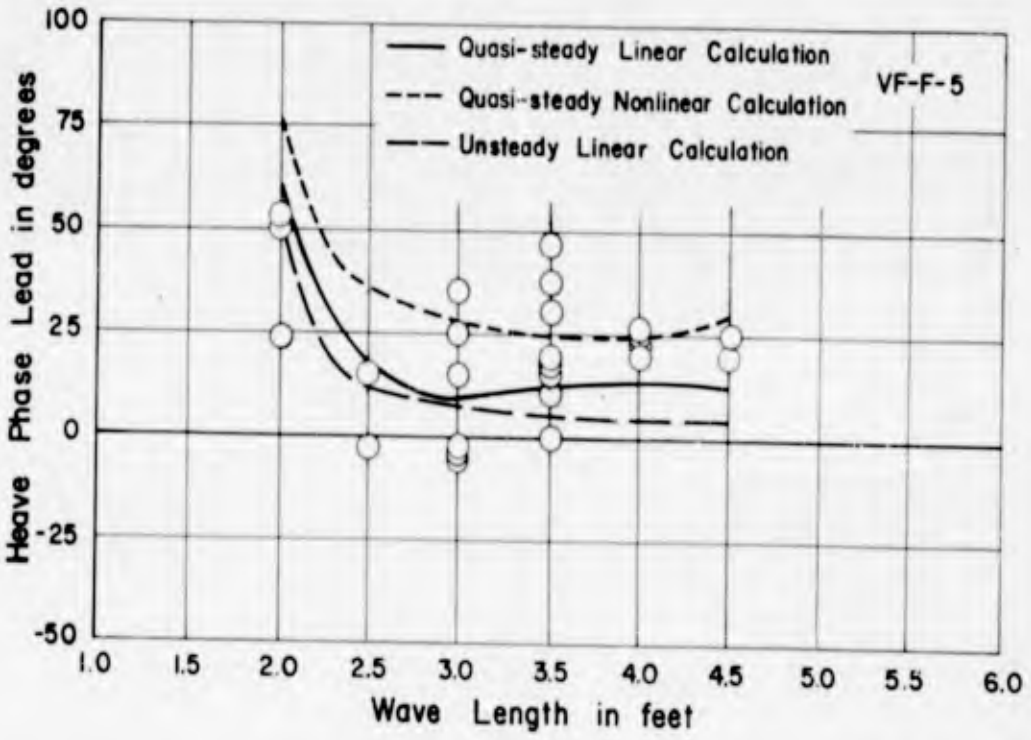

Fig. 8 - VF-F-5 Heave Response

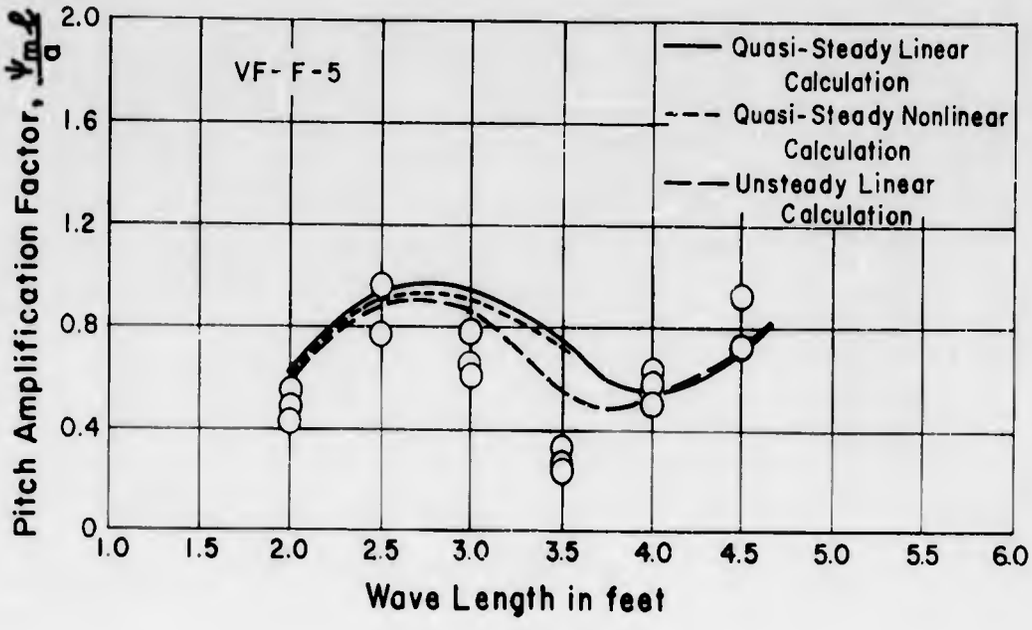

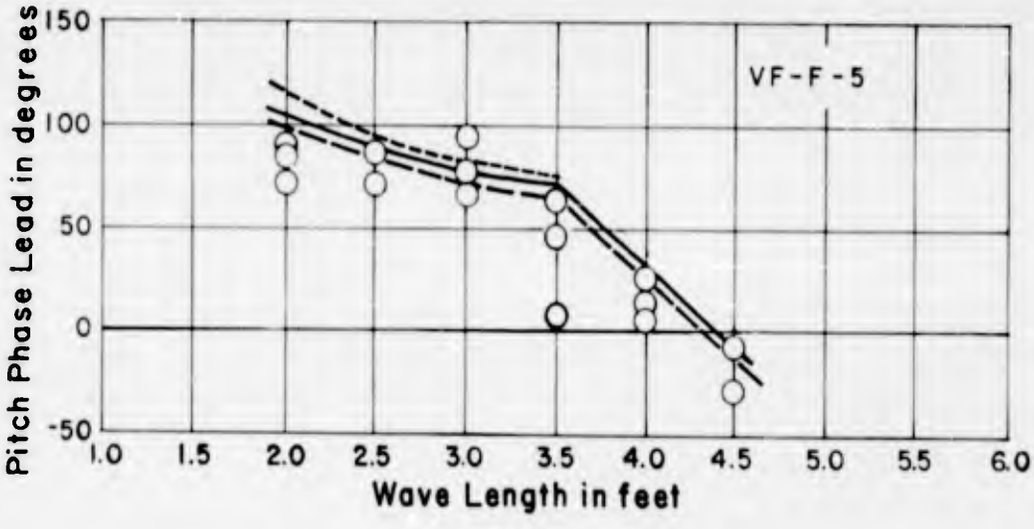

Fig. 9 – VF-F-5 Pitch Response

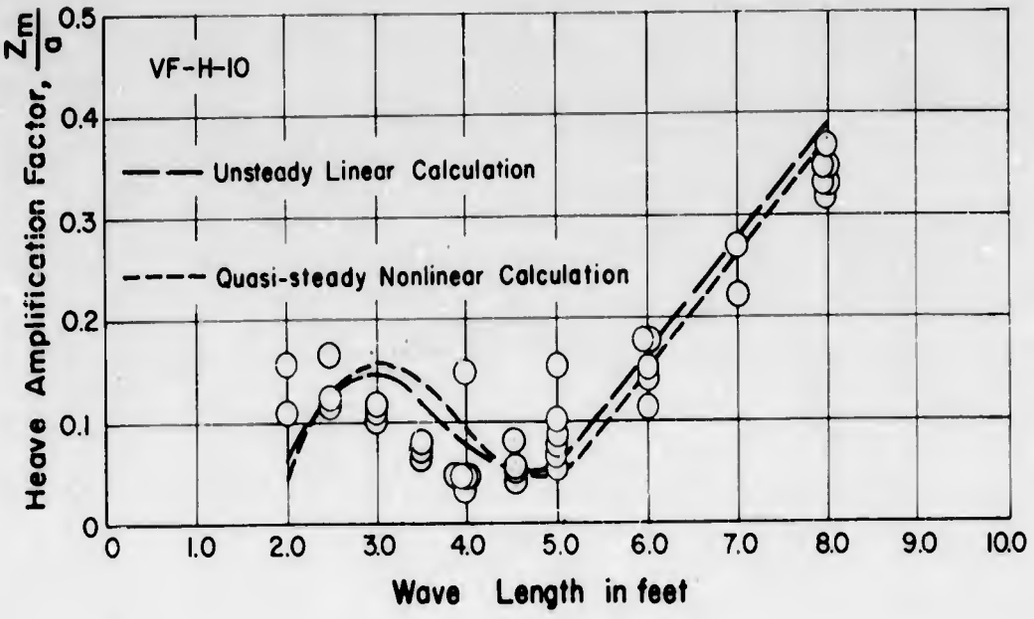

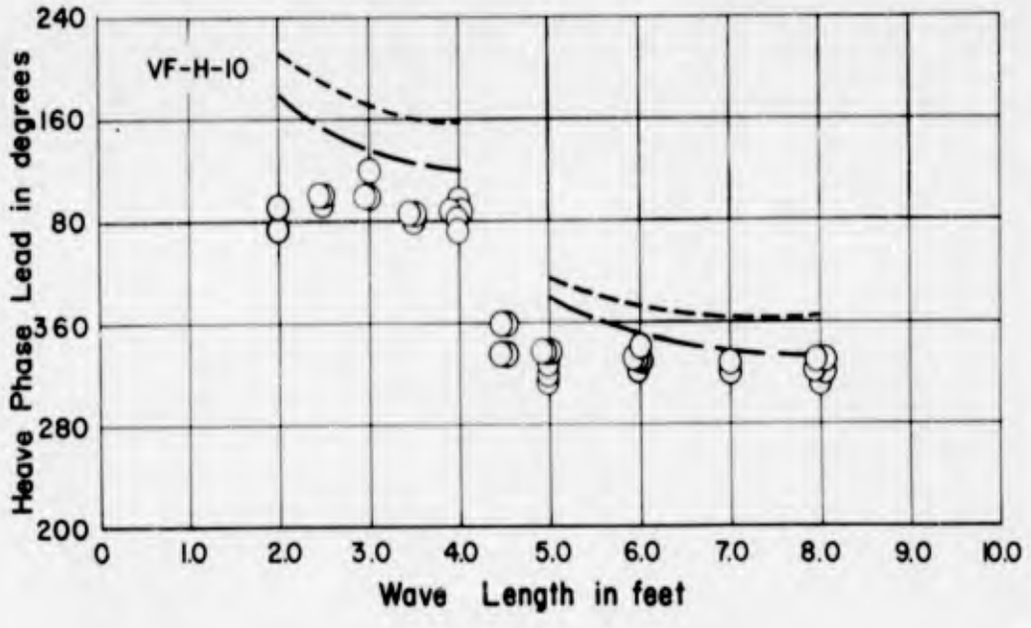

Fig. 10 - VF-H-10 Heave Response

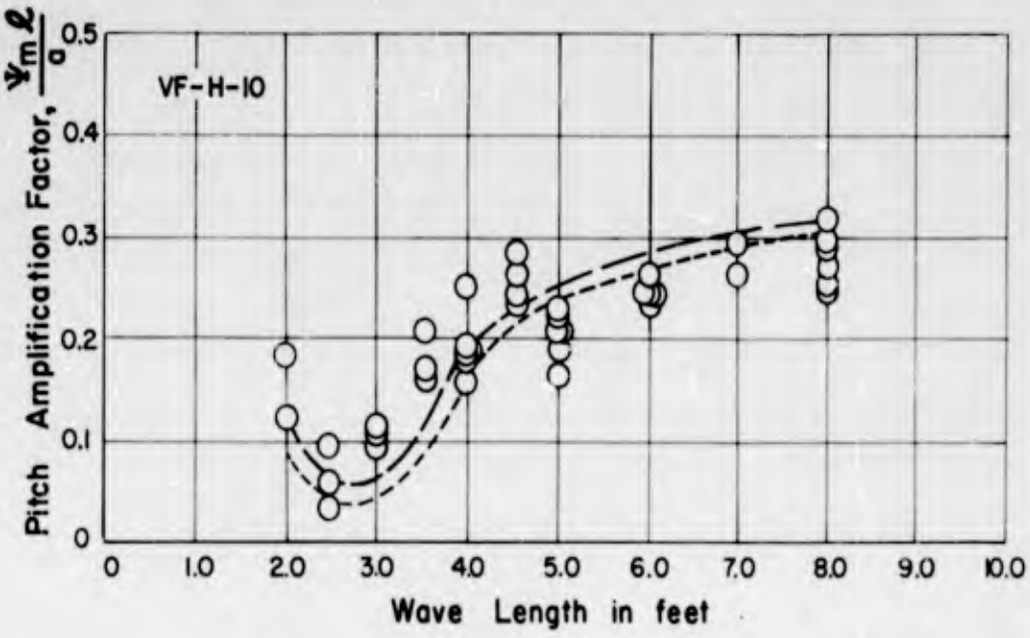

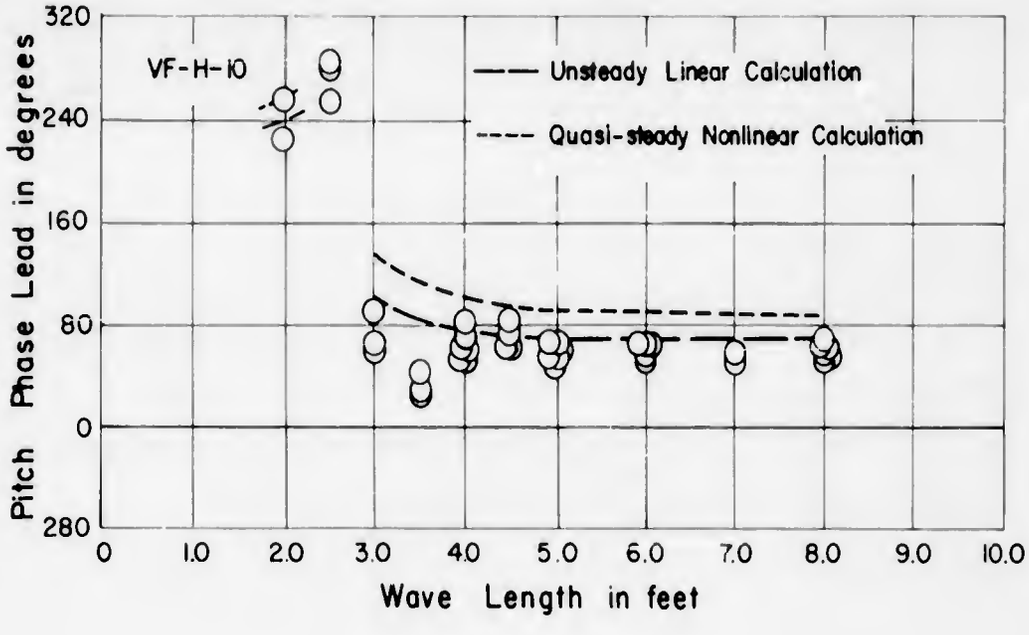

Fig. 11 - VF-H-10 Pitch Response

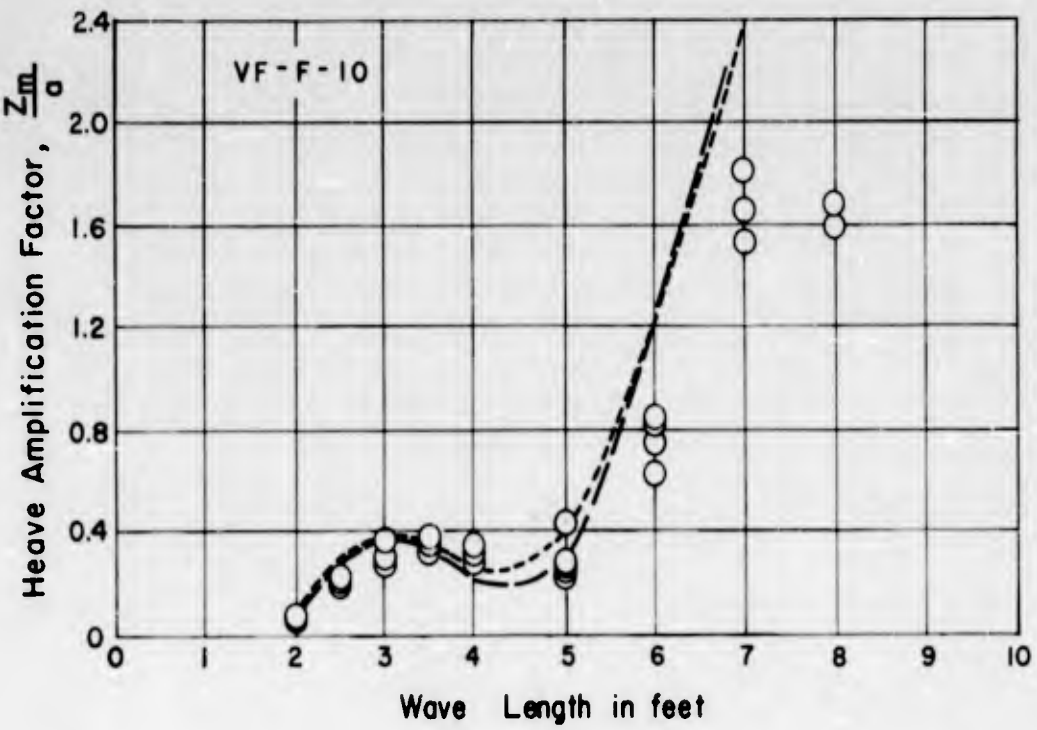

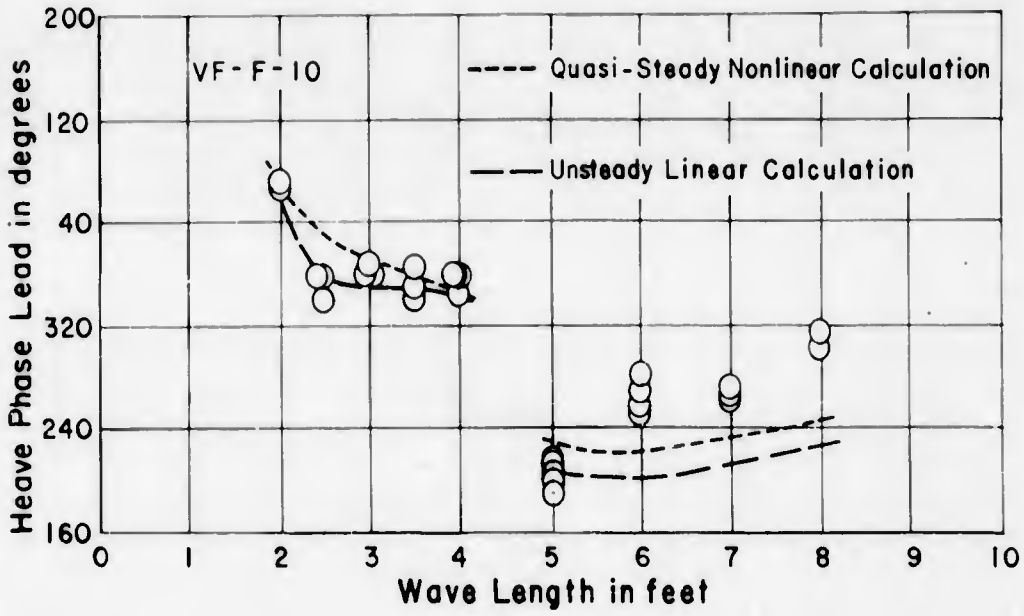

Fig. 12 - VF-F-10 Heave Response

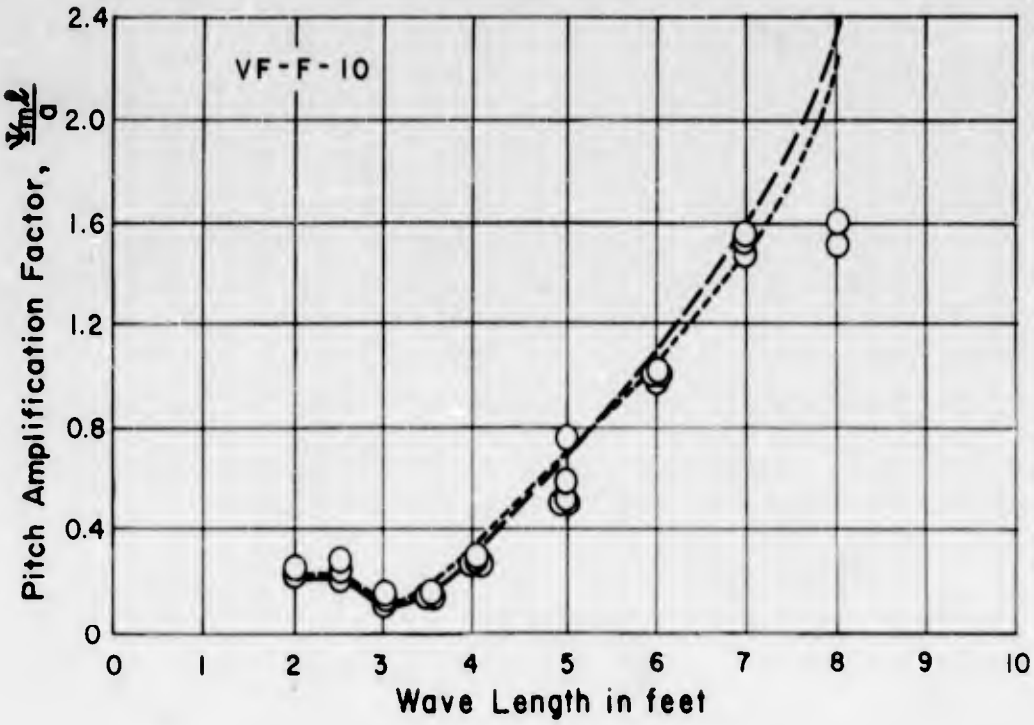

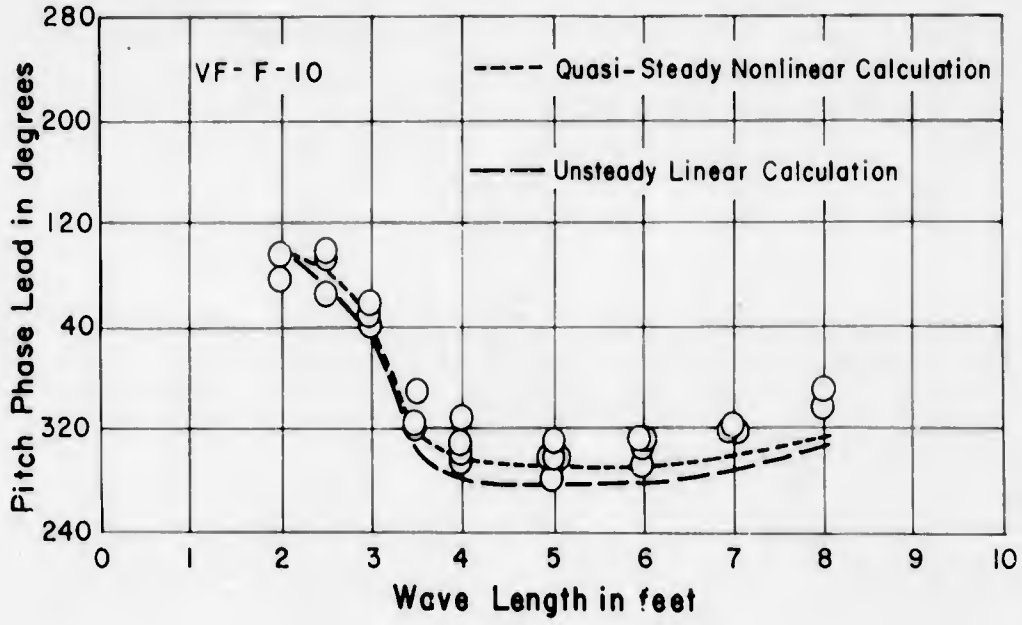

Fig. 13 - VF-F-10 Pitch Response

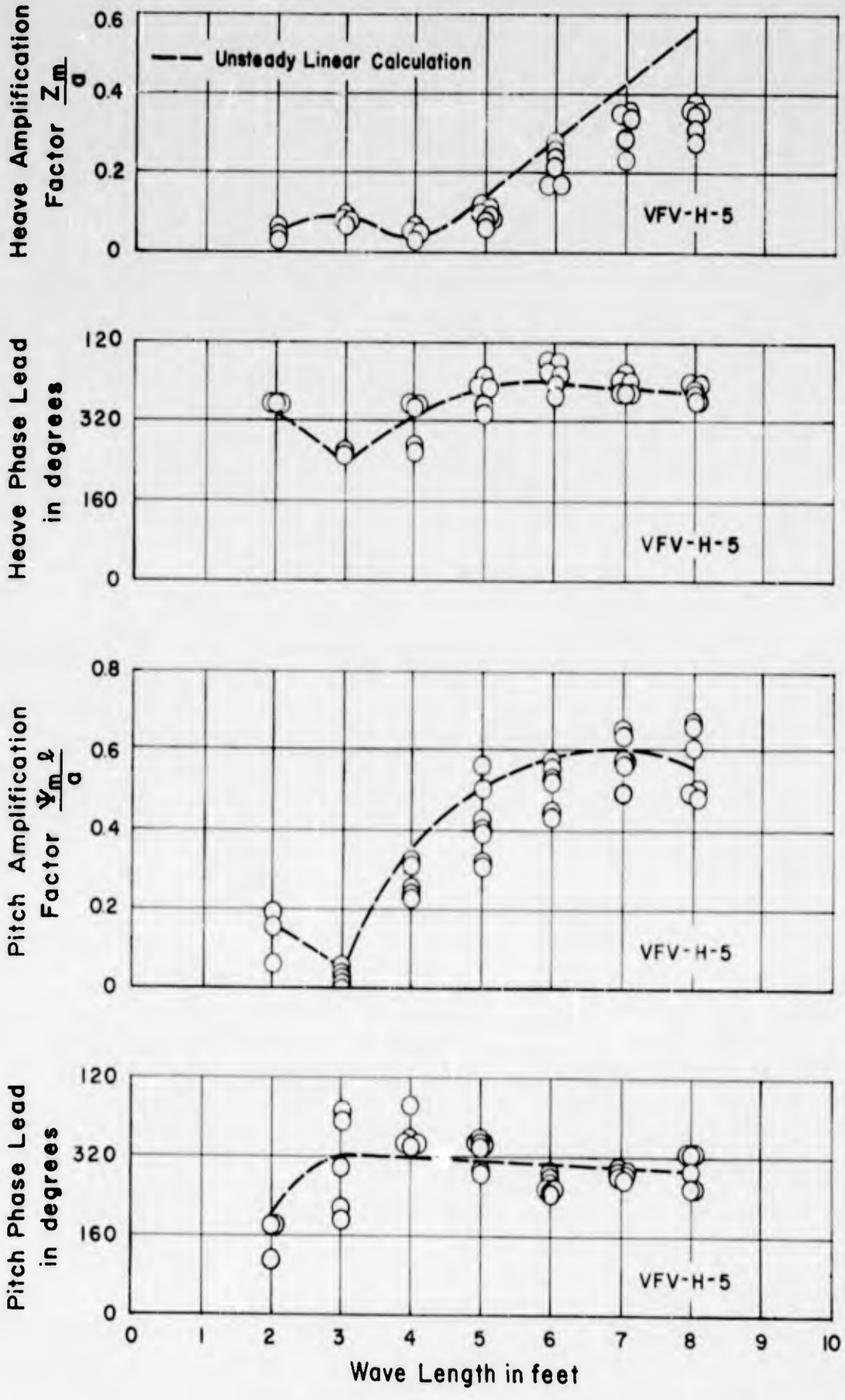

Fig. 14 - VFV-H-5 Heave and Pitch Responses

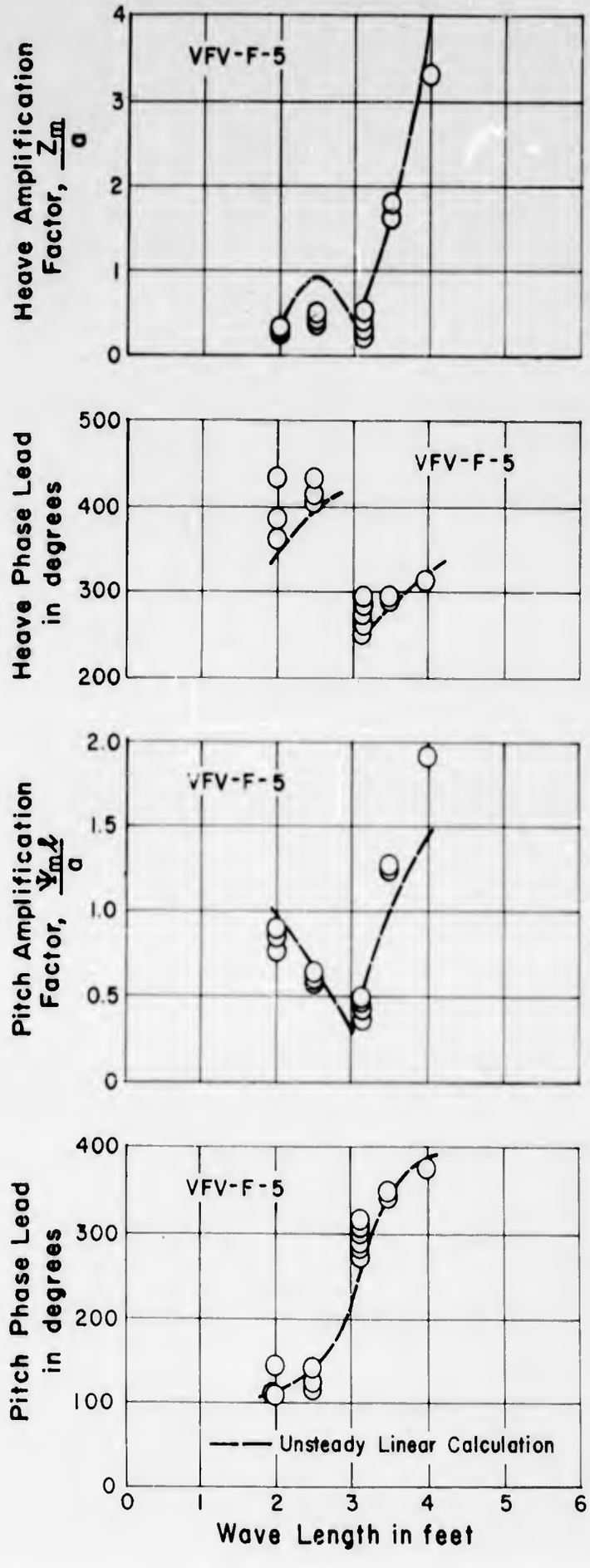

Fig. 15 - VFV-F-5 Heave and Pitch Responses

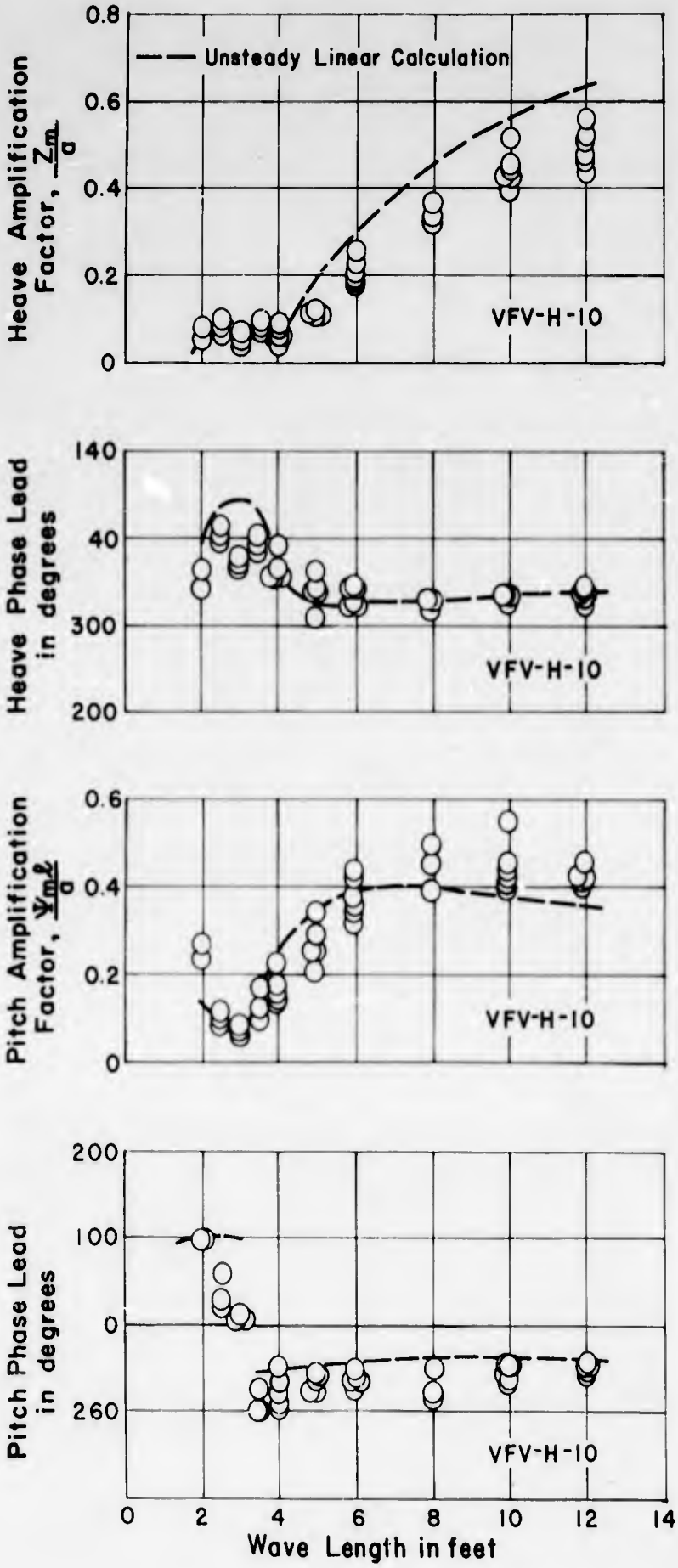

Fig. 16 - VFV-H-10 Heave and Pitch Responses

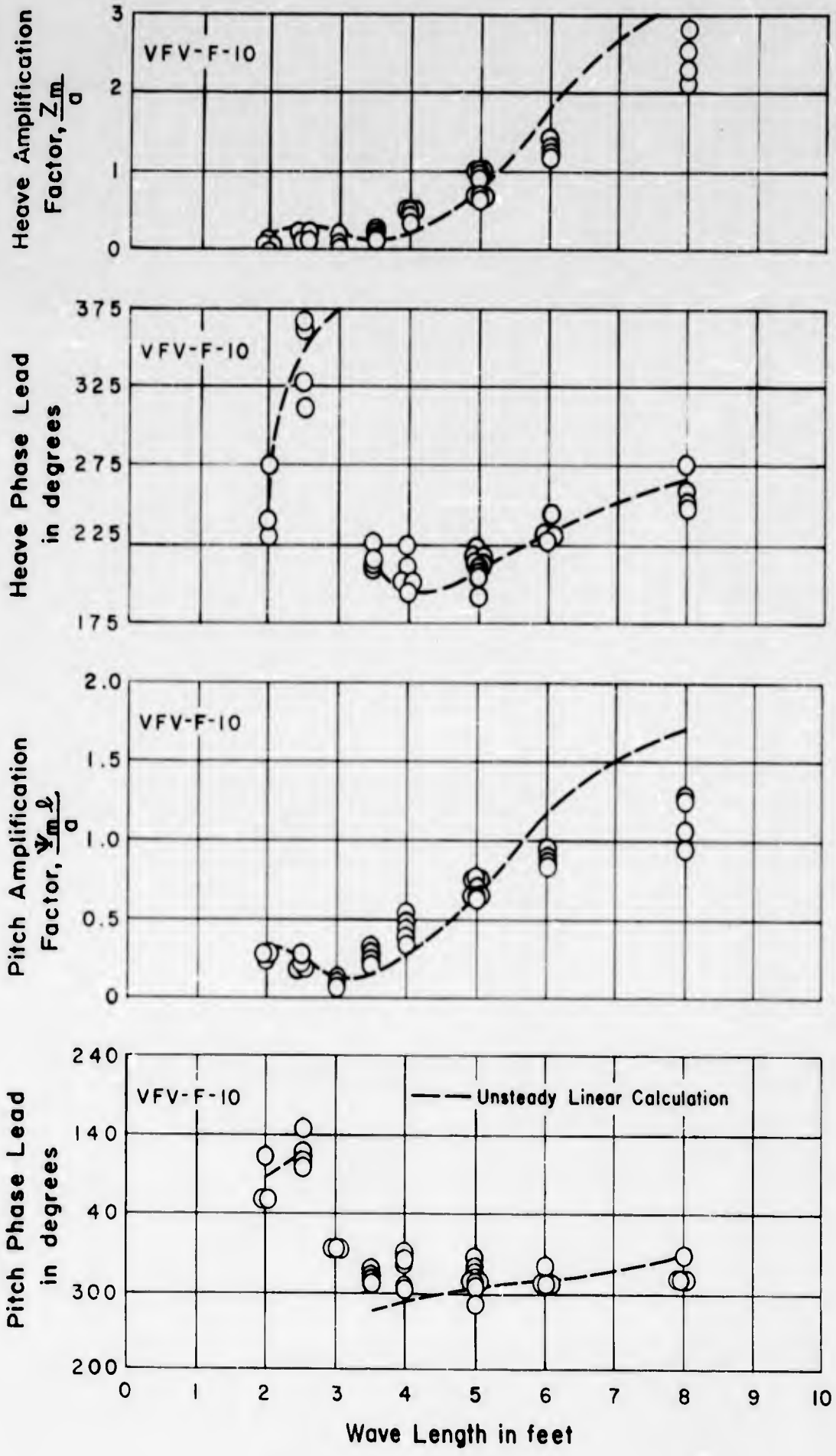

Fig. 17 - VFV-F-10 Heave and Pitch Responses

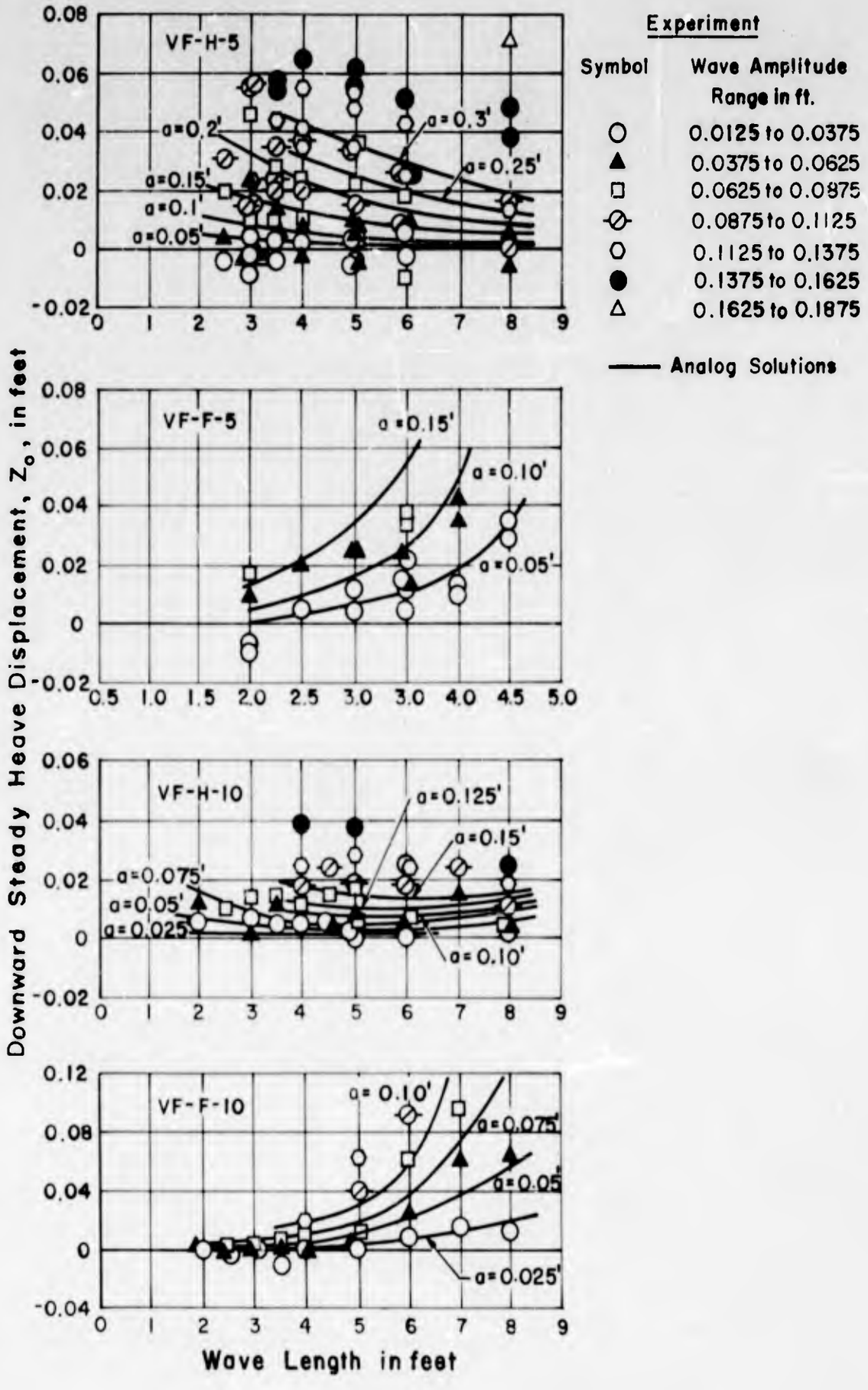

Fig: 18 - Steady Downward Component of Heave, VF Configuration

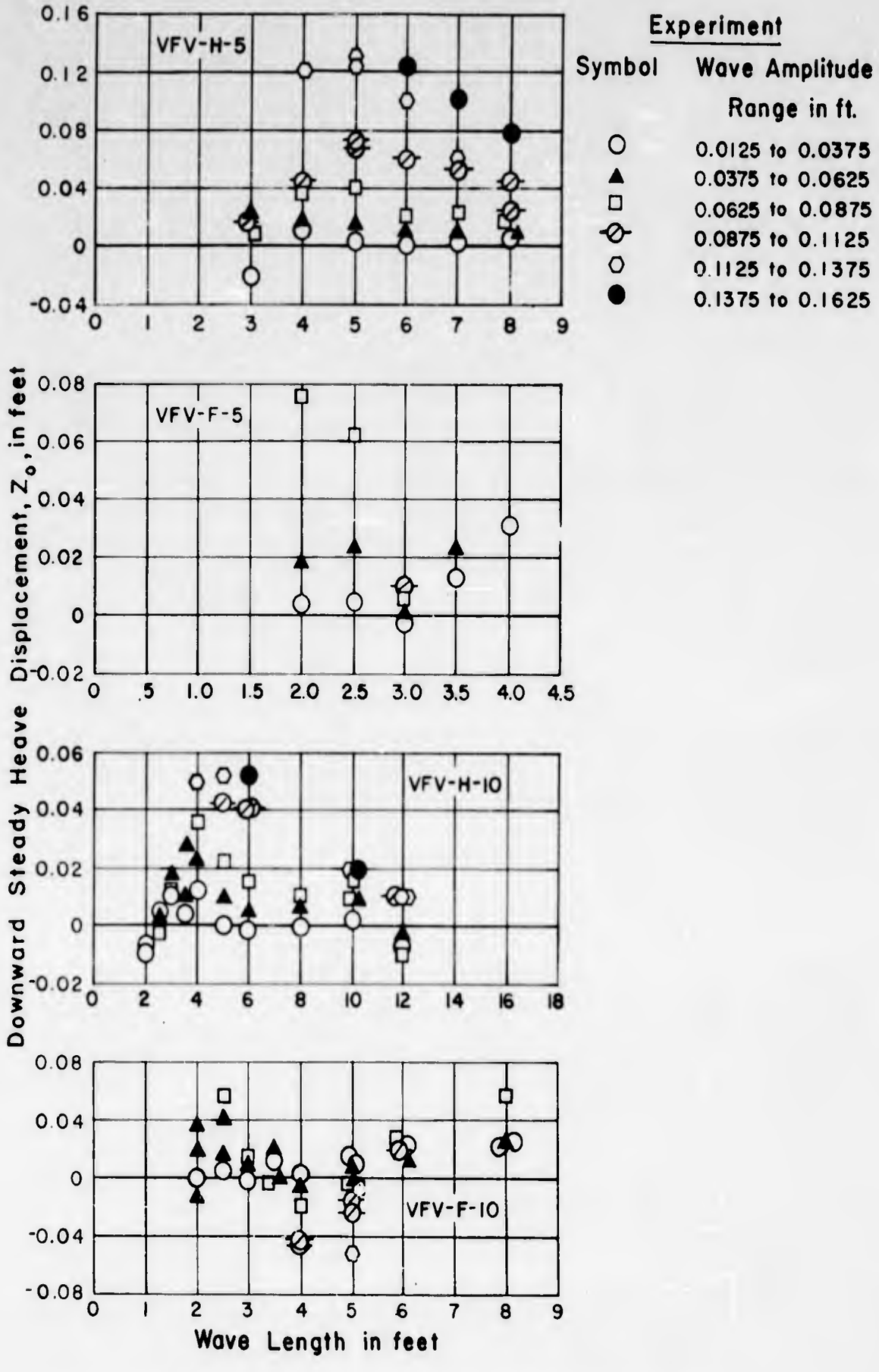

Fig. 19 - Steady Downward Component of Heave, VFV Configuration

APPENDIX A

LINEAR AND NONLINEAR QUASI-STEADY SOLUTIONS AND UNSTEADY LINEAR SOLUTIONS OF EQUATIONS OF MOTION

APPENDIX A

LINEAR AND NONLINEAR QUASI-STEADY SOLUTIONS AND UNSTEADY LINEAR SOLUTIONS OF EQUATIONS OF MOTION

A. Notation

The linearized equations, obtained by omitting all squared terms and cross products of the variables z, ψ, a and their derivatives, are presented here for reference purposes. The equations and solutions are presented in a general form which may be reduced to either the quasi-steady or unsteady form.

The following notation is defined for use in interpretation of the general solutions:

$\Delta = 1$ for V foils
$\Delta = 0$ for flat foils

$B_o = c_o \rho b V^2 \cot \mu$
$B' = c' \rho b V^2 \cot \mu$ for V foils

$F_o = 1/2\ \rho V^2\ c\ c_o$
$F' = 1/2\ \rho V^2\ c\ c'$ for flat foils

$\delta = +1$ for a foil forward of craft center of gravity
$\delta = -1$ for a foil aft of craft center of gravity

Where alternative signs are indicated the upper sign always refers to head seas and the lower sign to following seas.

The towing arm correction, which is discussed in Appendix B, is

$$T_2 = \frac{m}{m + I_T/\ell_T^2}$$

Also

$\beta_o = B_o d$ for V foils
$\beta_o = F_o s$ for flat foils
$\beta' = B' d$ for V foils
$\beta' = F' s$ for flat foils

$$A_o = \frac{1 - e^{-kd}}{kd} \quad \text{for V foils}$$

$$A_o = e^{-k\xi} \quad \text{for flat foils}$$

x = horizontal distance from the foil to the center of gravity of the craft (either e or ℓ depending on the configuration)

The general equations of motion are:

$$\frac{m\ddot{z}}{T_2} = \Sigma L - W \tag{A-1}$$

$$I\ddot{\psi} = \Sigma L\delta x \tag{A-2}$$

Upon insertion of the proper expressions for the lift in the above equations, the coupled equations of motion are obtained. The general equations will be written, considering unsteadiness effects, which can be removed to obtain the steady solutions.

B. Correction for Unsteadiness Effects

Unsteadiness is assumed to affect the lift on the foil through wake vorticity, added mass, and nonuniformity of the velocity over the chord due to the orbital motion. From analogy with the problem of oscillatory airfoils in aerodynamics, it is assumed that solutions exist of the form

$$z = Z e^{i\nu t}$$

$$\psi = \Psi e^{i\nu t} \tag{A-3}$$

where both Z and Ψ may be complex quantities. The expression for the lift is then written as the real part of

$$L = \beta_o + \frac{\beta'}{V}[V\Psi - i\nu Z - i\nu\delta x\Psi]D\, e^{i\nu t}$$

$$\pm \frac{\beta'}{V}[ia\omega A_o]Ee^{ik\delta x} e^{i\nu t} - \Delta B_o [Z + \delta x\Psi - ae^{ik\delta x}]e^{i\nu t} \tag{A-4}$$

D and E are unsteady force coefficients defined by

$$D = [C(\nu b/2V) + i\, \nu b/4V)] = Xe^{i\zeta}$$

$$E = [J_o(kb/2) - i\, J_1(kb/2)]C(\nu b/2V) + i\left[\frac{V \pm c}{V}\right] J_1(kb/2) = Ye^{i\theta}$$

$$C(\nu b/2V) = F(\nu b/2V) + iG(\nu b/2V) \quad \text{(Theodorsen's Function)}$$

J_o and J_1 are the Bessel functions of the first kind of order zero and one respectively. Plots of C, D, and E are shown in Figs. A-1 through A-4 for the range of conditions of interest. The Theodorsen function is plotted from values given in Reference [10]. The functions D and E reduce to one for the quasi-steady case. The complex function, D, can be divided into two parts: the wake vorticity correction C, and the added mass correction. Thus, the difference between the functions C and D for a particular reduced frequency represents the effect of added mass. The Theodorsen function, C, approaches the value 1/2 at large $\nu b/2V$, whereas D continues to change, indicating continued added mass effects. For a given foil and velocity, the wave length will increase with decreasing reduced frequency, indicating that added mass effects are more predominant for the smaller wave lengths.

The unsteady force function, E, corrects for nonuniformity of the velocity over the chord. As a term with an alternative sign appears, E will attain different values for head and following seas. These are presented in Figs. A-3 and A-4.

C. Solution of the General Equations

Substitution of Eqs. (A-3) and (A-4) into the equations of motion, (A-1) and (A-2), and subsequent linearization, gives:

$$Z(A_1 + i\, B_1) + \Psi(C_1 + i\, D_1) = E_1 + i\, F_1 \qquad \text{(A-5)}$$

$$A(A_2 + i\, B_2) + \Psi(C_2 + i\, D_2) = E_2 + i\, F_2 \qquad \text{(A-6)}$$

where

$$A_1 = -\frac{m\nu^2}{T_2} - \left(\frac{X\nu}{V} \sin\zeta\right) \Sigma \beta' + \Sigma \Delta B_o$$

$$B_1 = \left(\frac{X\nu}{V}\right) \cos\zeta) \Sigma\ \beta'$$

$$C_1 = -(X \cos\zeta)\,\Sigma\,\beta' - \left(\frac{X\nu}{V} \sin\zeta\right)\ \Sigma(\beta\,\delta x) + \Sigma(\Delta B_o \delta x)$$

$$D_1 = -(X \sin\zeta)\,\Sigma\,\beta' + \left(\frac{X\nu}{V} \cos\zeta\right)\Sigma(\beta'\delta x)$$

$$E_1 = \mp \left(\frac{a\omega Y}{V}\right)\,\Sigma\,(\beta' A_o \sin(\theta + k\delta x)) + a\,\Sigma(\Delta B_o \cos k\delta x)$$

$$F_1 = \pm \frac{a\omega Y}{V}\ \Sigma\,(\beta' A_o \cos(\theta + k\delta x)) + a\,\Sigma(\Delta B_o \sin k\delta x)$$

$$A_2 = -\left(\frac{X\nu}{V} \sin\zeta\right)\ \Sigma(\beta'\delta x) + \Sigma(\Delta B_o \delta x)$$

$$B_2 = \left(\frac{X\nu}{V} \cos\zeta\right(\ \Sigma\,(\beta'\delta x)$$

$$C_2 = -I\nu^2 - (X \cos\zeta)\ \Sigma(\beta'\delta x) - \left(\frac{X\nu}{V} \sin\zeta\right)\ \Sigma(\beta' x^2) + \Sigma(\Delta B_o x^2)$$

$$D_2 = -(X \sin\zeta)\ \Sigma(\beta'\delta x) + \left(\frac{X\nu}{V} \cos\zeta\right)\ \Sigma(\beta' x^2)$$

$$E_2 = \mp \frac{a\omega Y}{V}\ \Sigma(\beta' A_o \delta x \sin(\theta + k\delta x)) + a\,\Sigma(\Delta B_o \delta x \cos k\delta x)$$

$$F_2 = \pm \frac{a\omega Y}{V}\ \Sigma(\beta' A_o \delta x \cos(\theta + k\delta x)) + a\,\Sigma(\Delta B_o \delta x \sin k\delta x)$$

For the quasi-steady solution $X = Y = 1$ and $\zeta = \theta = 0$.

Equations (A-5) and (A-6) may then be solved using determinants. Let

$$Z = \frac{\nabla Z}{\nabla} \quad \text{and} \quad \Psi = \frac{\nabla \Psi}{\nabla}$$

where $$\nabla = \begin{vmatrix} A_1 + i\,B_1 & C_1 + i\,D_1 \\ A_2 + i\,B_2 & C_2 + i\,D_2 \end{vmatrix}$$

$$= A_3 + i\,B_3$$

where $A_3 = A_1C_2 - B_1D_2 - A_2C_1 + B_2D_1$

and $B_3 = A_1D_2 + B_1C_2 - A_2D_1 - B_2C_1$

$$\nabla Z = \begin{vmatrix} E_1 + i F_1 & C_1 + i D_1 \\ E_2 + i F_2 & C_2 + i D_2 \end{vmatrix}$$

$$= A_4 + i B_4$$

where $A_4 = E_1C_2 - F_1D_2 - C_1E_2 + D_1F_2$

and $B_4 = E_1D_2 + F_1C_2 - C_1F_2 - D_1E_2$

$$\nabla \Psi = \begin{vmatrix} A_1 + i B_1 & E_1 + i F_1 \\ A_2 + i B_2 & E_2 + i F_2 \end{vmatrix}$$

$$= A_5 + i B_5$$

where $A_5 = A_1E_2 - B_1F_2 - E_1A_2 + F_1B_2$

and $B_5 = A_1F_2 + B_1E_2 - B_2E_1 - F_1A_2$

Then $$Z = \frac{A_4 + i B_4}{A_3 + i B_3} = \frac{A_6 + i B_6}{A_3^2 + B_3^2}$$

Hence the dimensionless heave amplification factor,

$$\frac{Z}{a} = \frac{1}{a} \cdot \frac{\sqrt{A_6^2 + B_6^2}}{A_3^2 + B_3^2} \qquad \text{(A-7)}$$

and the heave phase lead

$$\phi_z = \tan^{-1} \frac{B_6}{A_6} \qquad \text{(A-8)}$$

where $A_6 = A_4A_3 + B_4B_3$

and $B_6 = B_4A_3 - A_4B_3$

Also $$\Psi = \frac{A_5 + i B_5}{A_3^2 + B_3^2} = \frac{A_7 + i B_7}{A_3^2 + B_3^2}$$

Hence, the dimensionless pitch amplification factor,

$$\frac{|\Psi|\ell}{a} = \frac{\ell}{a} \cdot \frac{\sqrt{A_7^2 + B_7^2}}{A_3^2 + B_3^2} \tag{A-9}$$

and the pitch phase lead.

$$\phi_\psi = \tan^{-1} \frac{B_7}{A_7} \tag{A-10}$$

where $A_7 = A_5A_3 + B_5B_3$

and $B_7 = A_3B_5 - B_3A_5$

The solutions of the linearized equations can be divided into two parts: the steady-state solution created by the periodic forcing function, which has been considered in this section, and the damped transient solution depending on the initial conditions, which will be considered in the next section.

Since a, the wave amplitude, may be factored in E_1, F_1, E_2, and F_2 it can be seen that it may also be factored from A_4, B_4, A_5, and B_5 and hence from A_6, B_6, A_7, and B_7. Finally, then, it may be factored from $|Z|$ and $|\Psi|$. Consequently, the dimensionless heave and pitch amplification factors are independent of the wave amplitude.

D. Transient Solutions and Stability

In order to determine the inherent stability of the configurations the homogeneous quasi-steady linearized solutions are used. These are presented in a different form than that used to find the steady-state solutions.

Again, omitting all squared terms and cross products of the variables a, ψ, a and their derivatives, the following equations are obtained:

$$\ddot{z} + A_8 \dot{z} + B_8 z + C_8\dot{\psi} + D_8\psi = E_8 \sin \nu t + F_8 \cos \nu t \tag{A-11}$$

$$\ddot{\psi} + A_9 \dot{\psi} + B_9\psi + C_9 \dot{z} + D_9 = E_9 \sin \nu t + F_9 \cos \nu t \tag{A-12}$$

The expressions on the right-hand side represent the forcing functions which are made equal to zero in order to obtain the transient solution.

Hence:

$$\ddot{z} + A_8 \dot{z} + B_8 z + C_8 \dot{\psi} + D_8 \psi = 0 \qquad \text{(A-13)}$$

$$\ddot{\psi} + A_9 \dot{\psi} + B_9 \psi + C_9 \dot{z} + D_9 z = 0 \qquad \text{(A-14)}$$

where

$$A_8 = \frac{1}{mV} \Sigma \beta'$$

$$B_8 = 1/m \Sigma (\Delta B_o)$$

$$C_8 = \frac{1}{mV} \Sigma (\beta' \delta x)$$

$$D_8 = -1/m \Sigma \beta' + 1/m \Sigma (\Delta B_o \delta x)$$

$$A_9 = 1/IV \Sigma (\beta' x^2)$$

$$B_9 = -1/I \Sigma (\beta' \delta x) + 1/I \Sigma (\Delta B_o x^2)$$

$$C_9 = 1/IV \Sigma (\beta' \delta x)$$

$$D_9 = 1/I \Sigma (\Delta B_o \delta x)$$

If solutions of the form $z = Ze^{\sigma t}$, $\psi = \Psi e^{\sigma t}$ are assumed to exist, then for the existence of non-trivial solutions it is necessary that the characteristic equation be

$$\sigma^4 + a_1\sigma^3 + a_2\sigma^2 + a_3\sigma + a_4 = 0 \qquad \text{(A-15)}$$

where $a_1 = A_8 + A_9$

$$a_2 = A_8A_9 + B_8 + B_9 - C_8C_9$$

$$a_3 = A_8A_9 + B_8A_9 - D_8C_9 - D_9C_8$$

$$a_4 = B_8B_9 - D_9D_8$$

The stability is guaranteed when the roots of the quartic (A-15) are negative or at most complex with negative real parts. This will be true if all the coefficients are greater than zero, and if Routh's discriminant

$$\Omega = a_1 a_2 a_3 - a_3^2 - a_1^2 a_4 > 0$$

The values of the coefficients, as well as the roots of the characteristic equation are given in Table A-I for each configuration and towing velocity used in the tests.

TABLE A-I

Coefficient or Root	Configuration			
	VF-5	VF-10	VFV-5	VFV-10
a_1	162	258	97	194
a_2	6,335	14,381	2,384	9,391
a_3	6,498	19,866	5,333	29,354
a_4	10,829	66,209	6,076	58,867
Ω	6.34×10^9	6.88×10^{10}	1.15×10^9	5.04×10^{10}
σ_1	-100.82	-0.645 + 2.04i	-1.175 + 1.20i	-113.18
σ_2	-61.20	-0.645 - 2.04i	-1.175 - 1.20i	-77.52
σ_3	-0.504 + 1.225i	-128.19 + 44.10i	-56.03	-1.605 + 2.033i
σ_4	-0.504 - 1.225i	-128.19 - 44.10i	-39.59	-1.605 - 2.033i

E. Analog Computer Solutions

Analog computer solutions were used to determine the theoretical steady heave component resulting from the nonlinearities. These were carried out for the VF configuration; insufficient time and funds prevented the completion of the solutions for the VFV configurations. A Reeve's Electronic Analog Computer (REAC) was used in this work. The linear solutions, previously obtained by hand computation, provided a check on the analog linear solutions. The REAC computer provides forty operational amplifiers and four independent servo multipliers each with three multiplying potentiometers.

For the VF configuration the quasi-steady nonlinear equations can be written in the form

$$\ddot{z} = P_1 \alpha_f + P_2 \alpha_a + P_3 \beta_f + P_4 \alpha_f \beta_f \qquad \text{(A-16)}$$

$$\ddot{\psi} = Q_1 \alpha_f - Q_2 \alpha_a + Q_3 \beta_f + Q_4 \alpha_f \beta_f \qquad \text{(A-17)}$$

where $P_1 = \dfrac{Bd_f}{m} c'_f$

$$P_2 = \frac{Bc'_a}{2m} s$$

$$P_3 = \frac{Bc_{o_f}}{m}$$

$$P_4 = \frac{Bc'_f}{m}$$

$$Q_1 = \frac{B\ell c'_f d_f}{I}$$

$$Q_2 = \frac{B\ell s c'_a}{2I}$$

$$Q_3 = \frac{B\ell c_{o_f}}{I}$$

$$Q_4 = \frac{B\ell c'_f}{I} \qquad \text{with } B = \rho b V^2$$

$$\alpha_f = \psi - \dot{z}/V - \ell\dot{\psi}/V + a R_1 \sin \nu t + a R_2 \cos \nu t \qquad \text{(A-18)}$$

where $R_1 = \mp \dfrac{\omega A_{o_f} \cos k\ell}{V}$ and $R_2 = \mp \dfrac{\omega A_{o_f} \sin k\ell}{V}$

$$\alpha_a = \psi - \dot{z}/V + \ell\dot{\psi}/V + a R_3 \sin \nu t + a R_4 \cos \nu t \qquad \text{(A-19)}$$

where $R_3 = \mp \dfrac{\omega e^{-kd_a} \cos k\ell}{V}$ and $R_4 = \pm \dfrac{\omega e^{-kd_a} \sin kl}{V}$

$$\beta_f = - z - \ell\psi + a R_5 \sin \nu t + a R_6 \cos \nu t \qquad \text{(A-20)}$$

where $R_5 = -\sin k\ell$ and $R_6 = \cos k\ell$

No expression for β_a appears since variation of lift with submergence was neglected in the case of flat foils.

These were then converted to machine equations as follows:

Computer time, $r = St = S \times$ real time

The computer variables are $[n_1 z]$, $[n_2 \dot{z}]$, $[n_3 \ddot{z}]$, $[n_4 \psi]$, $[n_5 \dot{\psi}]$, $[n_6 \ddot{\psi}]$, $[n_7 a_f]$, $[n_8 a_a]$, $[n_9 \beta_f]$, $[n_{10} \cos vr/S]$, and $[n_{10} \sin vr/S]$. These are chosen so that the maximum value of the computer variable will not exceed 100 volts. The n_i terms are the scale factors which satisfy this requirement. The machine equations become

$$\frac{[n_3 \ddot{z}]}{n_3} = p_1 \cdot \frac{[n_7 a_f]}{n_7} + p_2 \frac{[n_8 a_a]}{n_8} + \frac{[n_9 \beta_f]}{n_9}$$

$$+ p_4 \cdot \frac{[n_7 a_f]}{n_7} \cdot \frac{[n_9 \beta_f]}{n_9}$$

therefore $[n_3 \ddot{z}] = p_1 \frac{n_3}{n_7} [n_7 a_f] + p_2 \frac{n_3}{n_8} [n_8 a_a] + p_3 \frac{n_3}{n_9} [n_9 \beta_f]$

$$+ \frac{p_4 n_3 \cdot 100}{n_7 n_9} \frac{[n_7 a_f][n_9 \beta_f]}{100}$$

Note that $\int [n_3 \ddot{z}]\, dr = n_3 \dot{z} = \frac{n_3}{n_2} [n_2 \dot{z}]$

Hence

$$[n_2 \dot{z}] = \int \left\{ \frac{P_1}{n_2 n_7} [n_7 a_f] + \frac{P_2}{n_2 n_8} [n_8 a_a] + \frac{P_3}{n_2 n_9} [n_9 \beta_f] \right.$$

$$\left. + \frac{100\, P_4}{n_2 n_7 n_9} \cdot \frac{[n_7 a_f][n_9 \beta_f]}{100} \right\} dr$$

$$= \int \left\{ p_{15} g_{15} [n_7 a_f] + p_{16} g_{16} [n_8 a_a] + p_{17} g_{17} [n_9 \beta_f] \right.$$

$$\left. + p_{18} g_{18} \cdot \frac{[n_7 a_f][n_9 \beta_f]}{100} \right\} dr$$

where p_i = pot setting for pot i, and

g_i = gain on pot i output.

Similarly

$$[n_5 \dot{\psi}'] = \int \left| p_{19}g_{19}[n_7 a_f] - p_{20}\, g_{20}\, [n_8 a_a] + p_{21}g_{21}\, [n_9 \beta_f] + p_{22}g_{22}\, \frac{[n_7 a_f][n_6 \beta_f]}{100} \right| dr$$

$$[n_7 a_f] = p_1 g_1\, [n_4 \psi] - p_2 g_2\, [n_2 \dot{z}'] - p_3 g_3\, [n_5 \dot{\psi}'] + p_4 g_4\, [n_{10}\, a \sin \tfrac{vr}{S}] + p_5 g_5\, [n_{10}\, a \cos \tfrac{vr}{S}]$$

$$[n_9 \beta_f] = -p_6 g_6\, [n_1 z] - p_7 g_7\, [n_4 \psi] + p_8 g_8\, [n_{10}\, a \sin \tfrac{vr}{S}] + p_9 g_9\, [n_{10}\, a \cos \tfrac{vr}{S}]$$

$$[n_8 a_a] = p_{10}g_{10}\, [n_4 \psi] - p_{11}g_{11}\, [n_2 \dot{z}'] + p_{12}g_{12}\, [n_5 \dot{\psi}'] + p_{13}g_{13}\, [n_{10}\, a \sin \tfrac{vr}{S}] + p_{14}g_{14}\, [n_{10}\, a \cos \tfrac{vr}{S}]$$

The coefficients of the machine variables, n_i, and the pot settings and gains are shown in the following table for the two velocities and two conditions of encounter tested for the VF configuration.

The VFV configuration may be handled in a similar manner.

TABLE A-II

	VF-H-5	VF-F-5	VF-H-10	VF-F-10
$p_1 \times g_1$	0.050 x 1	0.500 x 1	0.260 x 1	0.625 x 1
$p_2 \times g_2$	0.250 x 4	0.975 x 4	0.260 x 4	0.594 x 4
$p_3 \times g_3$	0.375 x 4	0.408 x 10	0.156 x 10	0.891 x 4
$p_4 \times g_4$	$0.333R_1$ x 1	$0.250R_1$ x 1	$0.500R_1$ x 1	$0.500R_1$ x 1
$p_5 \times g_5$	$0.333R_2$ x 1	$0.250R_2$ x 1	$0.500R_2$ x 1	$0.500R_2$ x 1
$p_6 \times g_6$	0.130 x 1	0.938 x 4	0.208 x 1	0.563 x 1
$p_7 \times g_7$	0.195 x 1	0.450 x 4	0.078 x 4	0.211 x 4
$p_8 \times g_8$	$0.867R_6$ x 1	$0.600R_6$ x 1	$0.400R_6$ x 1	$0.450R_6$ x 1
$p_9 \times g_9$	$0.217R_5$ x 4	$0.600R_5$ x 1	$0.400R_5$ x 1	$0.450R_5$ x 1
$p_{10} \times g_{10}$	0.060 x 1	0.500 x 1	0.260 x 1	0.750 x 1
$p_{11} \times g_{11}$	0.300 x 4	0.975 x 4	0.260 x 4	0.713 x 4
$p_{12} \times g_{12}$	0.450 x 4	0.468 x 10	0.156 x 10	0.428 x 1
$p_{13} \times g_{13}$	$0.400R_3$ x 1	$0.250R_3$ x 1	$0.500R_3$ x 1	$0.600R_3$ x 1
$p_{14} \times g_{14}$	$0.400R_4$ x 1	$0.250R_4$ x 1	$0.500R_4$ x 1	$0.600R_4$ x 1
$p_{15} \times g_{15}$	0.738 x 4	0.607 x 4	0.789 x 4	0.365 x 4
$p_{16} \times g_{16}$	0.714 x 4	0.704 x 4	0.658 x 10	0.633 x 4
$p_{17} \times g_{17}$	0.237 x 1	0.211 x 1	0.565 x 1	0.232 x 1
$p_{18} \times g_{18}$	0.434 x 10	0.774 x 10	0.924 x 10	0.948 x 10
$p_{19} \times g_{19}$	0.758 x 4	0.779 x 4	0.811 x 4	0.430 x 4
$p_{20} \times g_{20}$	0.733 x 4	0.904 x 4	0.675 x 10	0.650 x 4
$p_{21} \times g_{21}$	0.243 x 1	0.271 x 1	0.580 x 1	0.238 x 1
$p_{22} \times g_{22}$	0.446 x 10	0.993 x 10	0.949 x 10	0.974 x 10
$p_{23} \times g_{23}$	0.025v x 4	0.321v x 1	0.025v x 4	0.105v x 1
$p_{24} \times g_{24}$	0.025v x 4	0.080v x 4	0.010v x 10	0.026v x 4
n_1	1000	16	480	80
n_2	100	4	120	20
n_3	10	4	30	5
n_4	1000	50	480	80
n_5	100	5	120	20
n_6	10	5	30	5
n_7	50	25	125	50
n_8	60	25	125	60
n_9	130	60	100	45
n_{10}	150	100	250	100
S	10	3.12	10	9.5

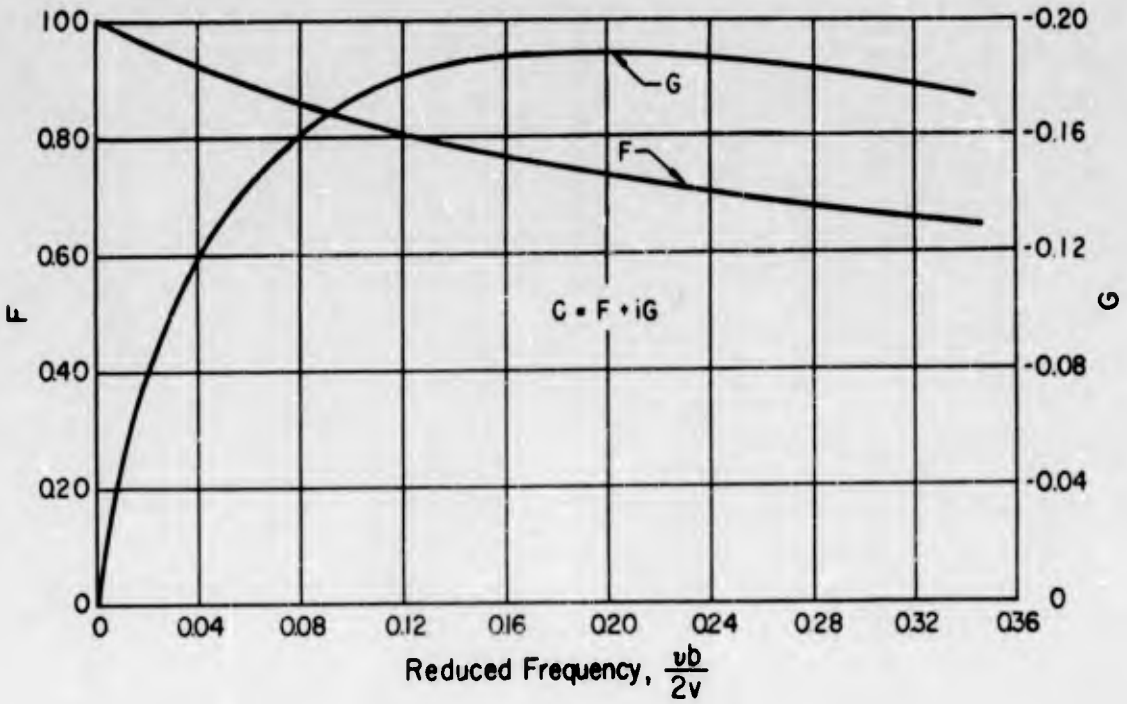

Fig. A-1 - Theodorsen's Function

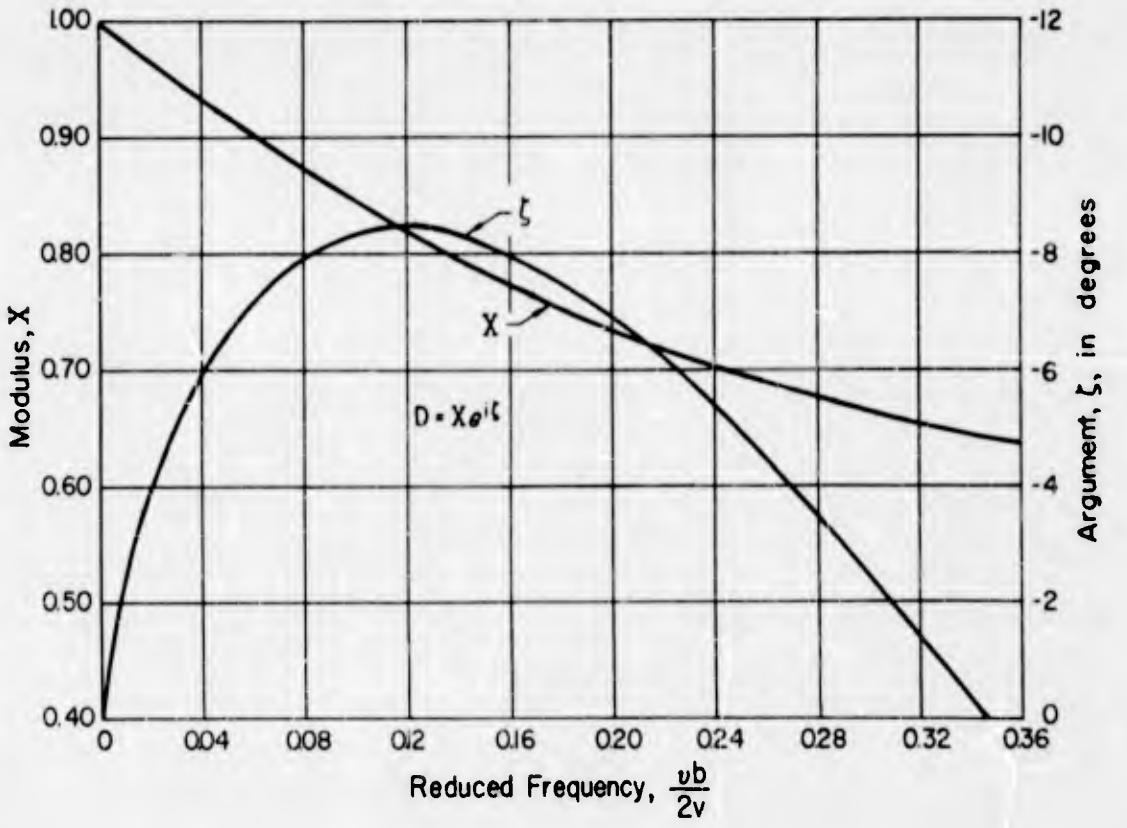

Fig. A-2 - Unsteady Force Function Considering Foil Motions

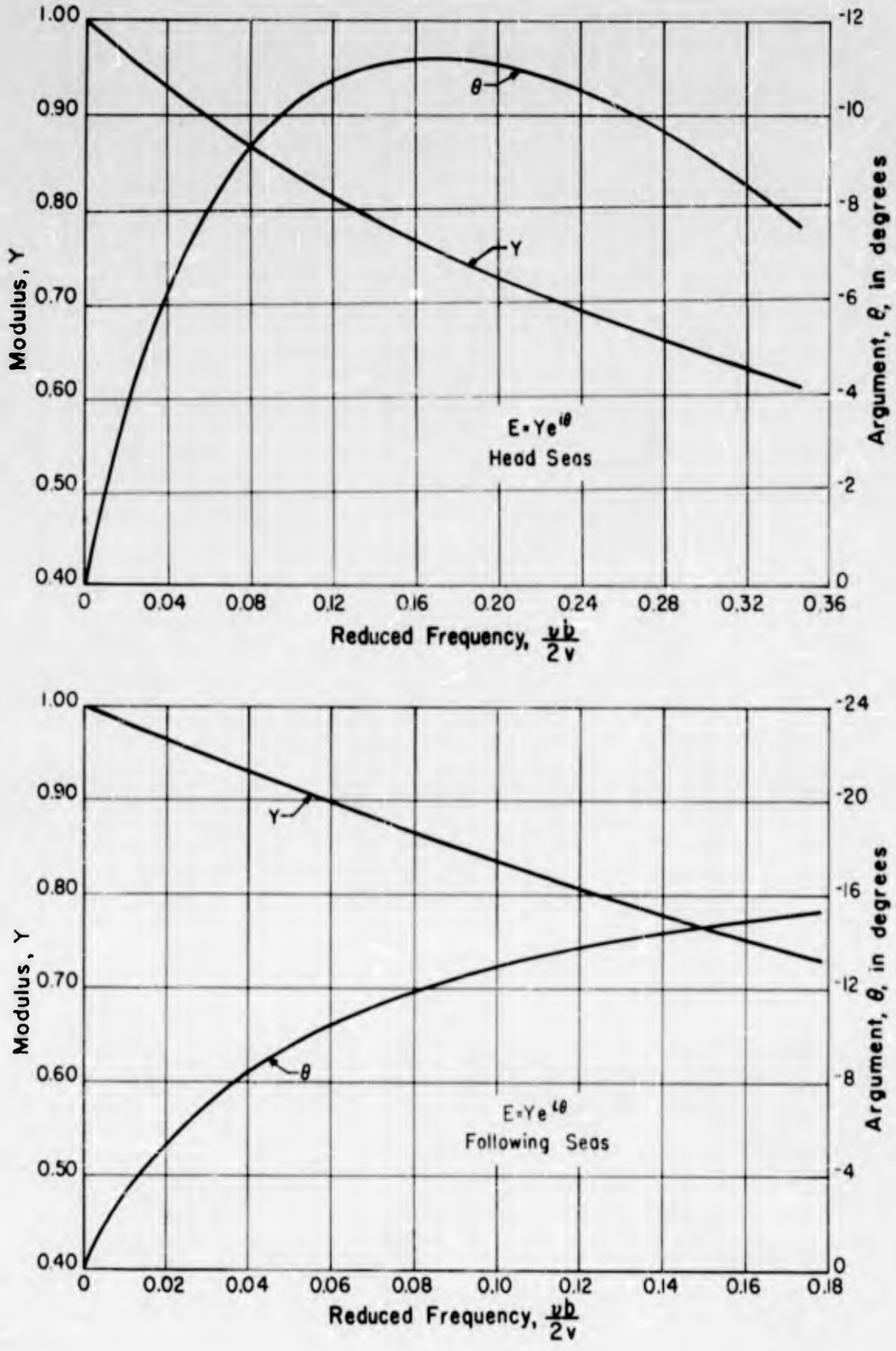

Fig. A-3 - Unsteady Force Functions Considering Nonuniformity of Velocity over Chord, V = 5 fps

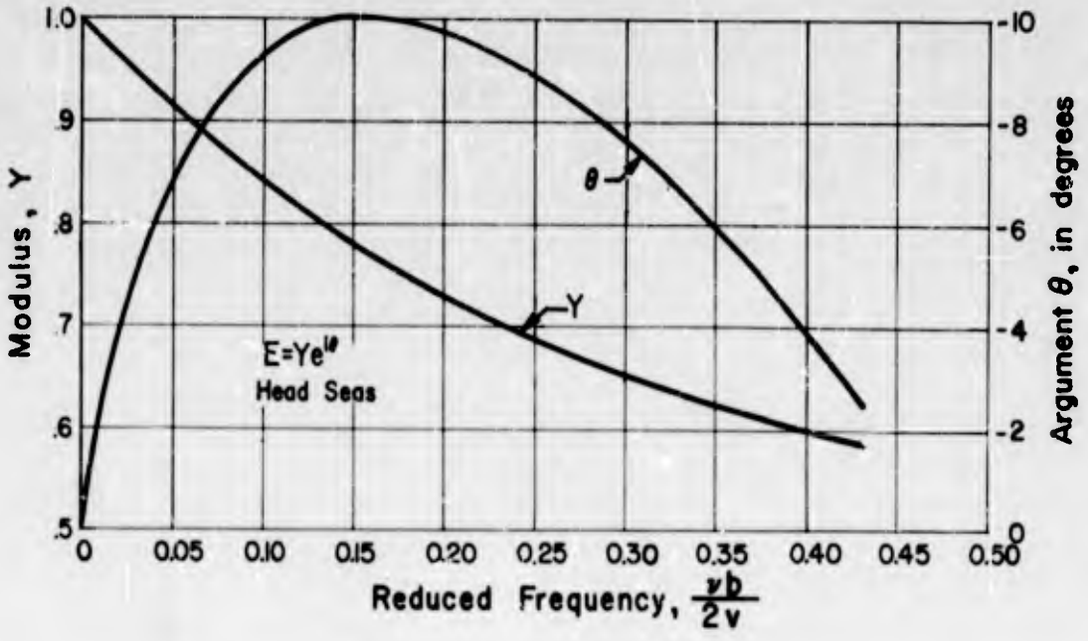

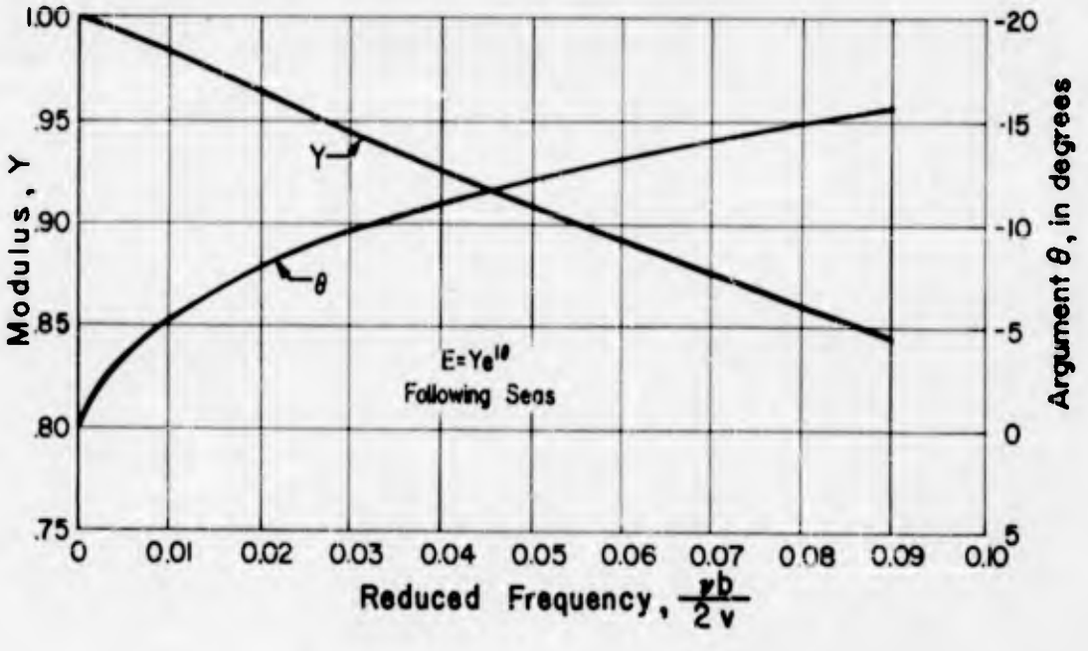

Fig. A-4 - Unsteady Force Functions Considering Nonuniformity of Velocity over Chord, V = 10 fps

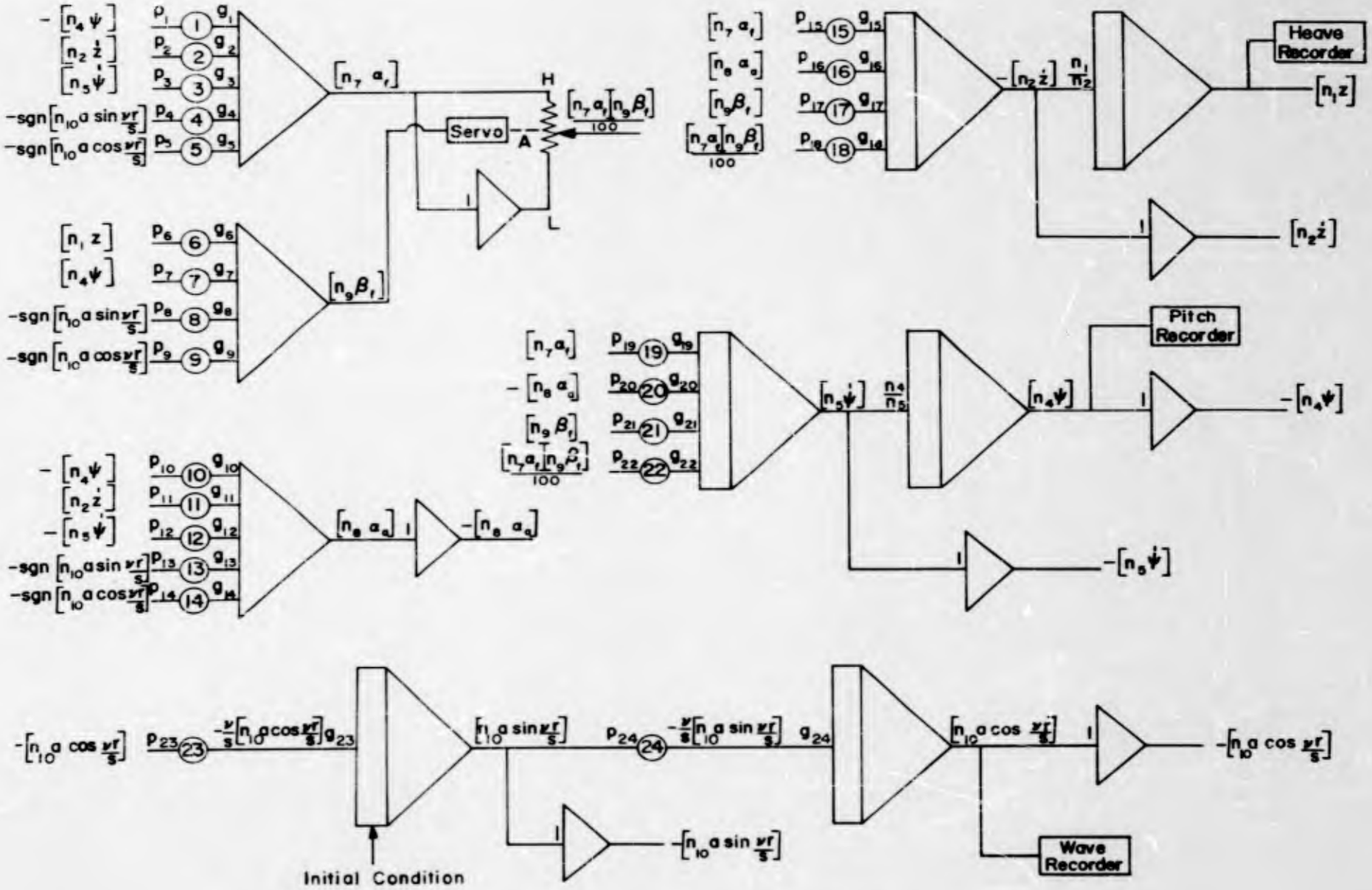

Fig. A-5 – Analog Computer Block Diagram, VF Configuration

APPENDIX B

TOWING ARM CORRECTION

APPENDIX B

TOWING ARM CORRECTION

As discussed in Section III-C, the weight of the towing arm was carefully balanced with the counterweight so that none of its weight bore on the craft. However, the inertia of the towing arm should be considered. The correction has been calculated by the method discussed by Leehey and Steele and reference will be made to Fig. 2.

As the craft is moved through a vertical distance Z, the towing arm will rotate about its axle through an angle θ. The equation describing such motion is

$$T = I\ddot{\theta} \tag{B-1}$$

If the length of the towing arm is ℓ_T, the torque, T, causing the rotation is given by

$$T = (\Sigma L - W)\ell_T \tag{B-2}$$

From the geometry, it can be seen that for small rotations

$$\theta \Omega Z/\ell_T$$

or

$$\ddot{\theta} \Omega \ddot{Z}/\ell_T \tag{B-3}$$

Then, combining Eqs. (B-1), (B-2), and (B-3)

$$\ddot{Z} = \frac{(\Sigma L - W)\ell_T^2}{I} \tag{B-4}$$

The moment of inertia, I, consists of the inertia of the towing arm, and that due to the mass of the craft. The moment about the pivot point of the towing arm is desired and can be obtained by the translation theorem.

Thus

$$m\ddot{Z} = \frac{(\Sigma L - W)m\,\ell_T^2}{I_T + m\,\ell_T^2} = \frac{(\Sigma L - W)\,m}{m + I_T/\ell_T^2} \tag{B-5}$$

This equation is the same as Eq. (A-1) where the factor T_2 is equal to

$$\frac{m}{m + I_T/\ell_T^2}$$

This factor then represents a correction to the fundamental equation of motion,

$$m\ddot{Z} = \Sigma L - W$$

from which the solutions are derived.

From Section C of Appendix A it is seen that the addition of the towing arm correction changes the heave computation only through the term A_1. In general, the influence of this correction is observed more significantly in the phase relationship.

APPENDIX C

HARMONIC ANALYSIS OF PITCH RESPONSE, VF-F-5

A P P E N D I X C

HARMONIC ANALYSIS OF PITCH RESPONSE, VF-F-5

Wave Length ft	Wave Height ft	Fundamental Pitch-Rads.	Second Harmonic / Fundamental	Third Harmonic / Fundamental
3.0	0.049	0.010	0.274	0.066
	0.089	0.030	0.320	0.128
	0.141	0.023	0.200	0.048
3.5	0.045	0.005	0.235	0.094
	0.060	0.005	0.131	0.200
	0.097	0.008	0.554	0.095
	0.148	0.011	0.880	0.276
4.0	0.048	0.010	0.363	0.088
	0.056	0.011	0.429	0.146
	0.089	0.015	0.389	0.144
4.5	0.049	0.012	0.161	0.111

SPONSOR'S DISTRIBUTION LIST FOR TECHNICAL PAPER NO. 37-B

of the St. Anthony Falls Hydraulic Laboratory

Copies	Organization
50	Commanding Officer and Director, David Taylor Model Basin, Washington 7, D. C., Attn: Code 513.
5	Chief of Naval Research, Department of the Navy, Washington 25, D. C., Attn: Code 438 and Code 439.
3	Chief of Naval Operations, Department of the Navy, Washington 25, D. C., Attn: 1 - Code OP-31 1 - Code OP-07 1 - Code OP-34
1	Commanding Officer, Office of Naval Research, Branch Office, 346 Broadway, New York 13, New York.
1	Commanding Officer, Office of Naval Research, Branch Office, The John Crerar Library Building, 10th Floor, 86 East Randolph Street, Chicago 1, Illinois.
1	Mr. R. K. Johnston, Miami Shipbuilding Corporation, 615 S. W. Second Avenue, Miami 36, Florida.
1	Director, U. S. Naval Research Laboratory, Washington 25, D. C.
1	Commandant, U. S. Marine Corps, Department of the Navy, Washington 25, D. C., Attn: G-3.
1	Assistant Chief of Transportation for Military Operations, Department of the Army, Washington, D. C.
1	Director, Army Research Office, Department of the Army, Washington 25, D. C.
1	Secretary, Undersea Warfare Committee, National Research Council, 2101 Constitution Avenue, N. W., Washington, D. C.
1	Mr. J. G. Baker, President, Baker Manufacturing Company, Evansville, Wisconsin.
1	Dr. L. G. Straub, Director, St. Anthony Falls Hydraulic Laboratory, University of Minnesota, Minneapolis 14, Minnesota.
10	Chief, Bureau of Ships, Department of the Navy, Washington 25, D. C., Attn: 3 - Technical Information Branch (Code 335) 1 - Ship Silencing (Code 345) 1 - Preliminary Design (Code 420) 1 - Hull Design (Code 440)

Copies	Organization
	1 - Scientific and Research (Code 442) 1 - Boats and Small Craft (Code 449) 1 - Mine, Service and Patrol Craft (Code 526) 1 - Landing Ships, Boats and Amphibious Vehicles (Code 529)
1	Chief, Bureau of Naval Weapons, Department of the Navy, Washington 25, D. C., Attn: Code RS.
1	Commanding Officer, Office of Naval Research, Branch Office, 495 Summer Street, Boston 10, Massachusetts.
1	Commanding Officer, Office of Naval Research, Branch Office, 1030 East Green Street, Pasadena 1, California
2	Commanding Officer, Office of Naval Research, Branch Office, Navy 100, F. P. O., New York, New York.
1	Director, National Aeronautics and Space Administration, 1512 H Street, N. W., Washington 25, D. C.
1	Commandant, U. S. Coast Guard, 1300 E Street, N. W., Washington 25, D. C.
1	Commandant, Marine Corps Schools, Quantico, Virginia, Attn: Marine Corps Development Center.
2	Director of Research and Development, Department of the Air Force, Washington 25, D. C.
1	Director, Weapons Systems Evaluation Group, Office of the Secretary of Defense, Washington 25, D. C.
1	Mr. T. M. Buerman, Gibbs and Cox, Incorporated, 21 West Street, New York 6, New York.
1	Commanding Officer, Office of Naval Research, Branch Office, 1000 Geary Street, San Francisco 9, California.
1	Professor H. A. Schade, Head, Department of Naval Architecture, University of California, Berkeley, California.
1	Dr. A. G. Strandhagen, Head, Department of Engineering Mechanics, University of Notre Dame, Notre Dame, Indiana.
1	Mr. W. R. Ryan, Edo Corporation, College Point 56, Long Island, New York.
1	Commander, Air Research and Development Command, P. O. Box 1395, Baltimore 3, Maryland, Attn: Rdtded.
10	Commander, Armed Services Technical Information Agency, Arlington Hall Station, Arlington 12, Virginia.

Copies	Organization
1	Mr. Phillip Eisenberg, President, Hydronautics, Incorporated, 200 Monroe Street, Rockville, Maryland.
1	Officer in Charge, MWDP Contract Supervisory Staff, SACLANT ASW Research Center, APO 19, New York, New York.
1	Dr. R. C. Seamans, Radio Corporation of America, Waltham, Massachusetts.
1	Hydrodynamics Research Laboratory, Consolidated-Vultee Aircraft Corporation, San Diego 12, California.
1	Mr. J. D. Pierson, The Martin Company, Baltimore 3, Maryland.
1	Dynamic Developments, Incorporated, Seaplane Hangar, Midway Avenue, Babylon, Long Island, New York.
1	Dr. M. S. Plesset, Hydrodynamics Laboratory, California Institute of Technology, Pasadena, California.
1	Commanding Officer and Director, U. S. Naval Civil Engineering Laboratory, Port Hueneme, California, Attn: Code L54.
1	Director, Davidson Laboratory, Stevens Institute of Technology, Hoboken, New Jersey.
1	Technical Research Group, 2 Aerial Way, Syosset, L. I., New York, N. Y., Attn: Dr. Jack Kotik.
1	Editor, Engineering Index, Inc., 29 West 39th Street, New York, N. Y.
1	Editor, Applied Mechanics Reviews, Southwest Research Institute, 8500 Culebra Road, San Antonio 6, Texas.
1	Librarian, Institute of Aeronautical Sciences, 2 East 64th Street, New York 21, New York.
1	Librarian, Society of Naval Architects and Marine Engineers, 74 Trinity Place, New York 6, New York.
1	Commander, U. S. Naval Ordnance Test Station, China Lake, California.
1	Commander, U. S. Naval Ordnance Test Station, Pasadena Annex, 3202 East Foothill Boulevard, Pasadena 8, California.
1	Mr. R. P. Godwin, Acting Chief, Office of Research and Development, Maritime Administration, 441 G Street, N. W., Washington, D. C.
1	Boeing Airplane Company, Seattle Division, Seattle, Washington.
1	Cornell Aeronautical Laboratory, Inc., Buffalo 21, New York.

Copies	Organization
1	Massachusetts Institute of Technology, Fluid Dynamics Research Laboratory, Cambridge, Massachusetts, Attn: Professor H. Ashley.
1	Dr. H. Norman Abramson, Director, Department of Mechanical Sciences, Southwest Research Institute, 8500 Culebra Road, San Antonio 6, Texas.
1	State University of Iowa, Iowa Institute of Hydraulic Research, Iowa City, Iowa, Attn: Professor L. Landweber.
1	Dr. Paul Kaplan, Oceanics, Incorporated, 114 East 40th Street, New York 16, New York.
1	Grumman Aircraft Engineering Corporation, Bethpage, L. I., New York. Attn: Mr. Leo Geyer.

UNCLASSIFIED